RSC Advances

ROYAL SOCIETY OF CHEMISTRY

www.rsc.org/advances

Biophysical, Biopharmaceutical and Toxicological Significance of Biomedical Nanoparticles

Sangeetha Aula[1,2], Samyuktha Lakkireddy[1,2], Kaiser Jamil[1], Atya Kapley[1,3], AVN Swamy[4], Harivardhan Reddy Lakkireddy[5*]

[1] Centre for Biotechnology and Bioinformatics, Jawaharlal Nehru Institute of Advanced Studies (JNIAS), Secunderabad, Telangana, India

[2] Department of Biotechnology, Jawaharlal Nehru Technological University Anantapur (JNTUA), Anantapuramu, Andhra Pradesh, India

[3]Environmental Genomics Division, Council of Scientific and Industrial Research- National Environmental Engineering Research Institute (CSIR-NEERI), Nagpur, Maharashtra, India.

[4]Department of Chemical Engineering, Jawaharlal Nehru Technological University Anantapur (JNTUA), Anantapuramu, Andhra Pradesh, India

[5] Drug Delivery Technologies and Innovation, Pharmaceutical Sciences, Sanofi Research and Development, 13 Quai Jules Guesde 94403 Vitry-sur-Seine, France

[*]Author for correspondance

Abstract

Nanotechnology has undoubtedly brought innovation to the biomedical field, which is apparent from the advances including in drug delivery, treatment of pathologies, imaging of disease sites, etc. The rationale behind the use of nanoparticle-based products for biomedical applications is to benefit from their unique physicochemical characteristics, such as, size, surface area and surface functionality, to address these particles and the encapsulated payload, if any, to the desired sites in the biological system. For designing appropriate nanoparticle products for biomedical applications aimed for human and/or animal use, understanding of the interplay between the physicochemistry of nanoparticles and the biophysical properties is crucial because it is the interaction of the nanoparticles at the biological interface which regulate the nanoparticles pharmacokinetics, biodistribution and safety. Also, the assessment of the potential of nanoparticles to induce undesired effects at the systemic level, organ level, cellular and sub-cellular levels is crucial for anticipating the potential risks associated with the use of nanoparticles from a safety standpoint. This review is aimed at summarizing the nanoparticles candidates for biomedical applications, and reviewing, based on the relevant literature data, the inter-relationship between nanoparticles' physicochemistry and biophysical properties in conditioning the nano-bio interactions and inturn regulating the nanoparticles pharmacokinetics, biodistribution and toxicological properties. Besides, the importance of designing of relevant physiologically-based modeling approaches for the simulation and prediction of performance and safety of new nanomaterials based on their properties has been also discussed. An important portion of the review focusses also on description of the methodologies for the detailed assessment of toxicological properties of the nanoparticles.

1. Introduction

Significant advances in nanotechnology in the field of biomedicine have resulted in a variety of smart innovations, especially in the areas of disease therapy and imaging, many of which have been transformed successfully into clinically applicable products. Biomedical nanotechnology has been an inter-disciplinary field orchestrated by physics, biology, chemistry, engineering, pharmacy, etc., to translate the idea from brain and bench to the bedside.

In disease therapy, the nanotechnology has an important contribution to the transformation of the way the drugs challenging from physicochemical and biopharmaceutical standpoints have been delivered, and also the treatment of pathologies using nanoparticles *per se*[1-3]. For imaging, nanotechnology has been successfully employed in clinical situations in imaging of various pathologies with improved performance[4-6]. Such successful milestones in biomedical nanotechnology have led to the continued motivation of researchers to design and explore a variety of new materials (e.g. polymers, lipids, inorganic materials, and hybrid composites), architectures, and functionalities for enhanced performance, responsive to different stimuli, compatible with biological milieu, etc. for addressing the evolving biomedical challenges, as evident from the intensive literature and intellectual property published each year in this area. While the performance of such new nanomaterials is important from their effectiveness standpoint, understanding of these nanomaterials with increasing complexity, from structural, physicochemical, biophysical, biopharmaceutical and toxicological standpoints, and their inter-play, is crucial to be able to develop performing and safer nanoparticle products and to ensure the product with reproducible quality attributes at each stage of development for intended application. Thus, in this review, we summarized the importance of the above aspects in the nano-bio interaction space, including the key considerations and assays for a detailed assessment of the toxicological properties of the nanoparticles, both in *in vitro* and in *in vivo* settings.

2. Nanoparticles for biomedical applications :

Biomedical nanotechnology, which involves the design and development of nanoparticles for various biomedical applications, has encountered a significant pace of development in the recent years as evident from a variety of nanotechnology-based products commercialized and in clinical and preclinical testing for biomedical purposes. The nanoparticles for biomedical applications could be classified as indicated in the Figure 1.

The principal applications for which the nanoparticles have been widely employed include the delivery of medicinal substances (prophylactic or therapeutic)[7,8], for disease therapy by local induction of stimuli in the target tissues[9,10], for imaging[11,6], for simultaneous therapy and imaging (termed as 'theranostic')[12,13], for tissue engineering[14], for detoxification[15,16], etc.

The main focus of nanoparticles application in the recent years has been on drug delivery (e.g. therapeutic agents, prophylactic agents, antigens, genes). This area has advanced significantly with the introduction of a variety of approaches to address specific challenges, such as, improvement of dissolution of poorly soluble drug molecules[17,18] enable the administration of poorly soluble drugs[19,20], alter the drug pharmacokinetics to achieve desired therapeutic efficacy and safety[21,22], site-specific delivery of the drugs to specific organs/tissues of interest[23-25], and enable the intracellular delivery of difficult-to-deliver drugs[26,27], such as, nucleic acids, proteins and peptides. In case of vaccines, the nanoparticles have been employed as carriers for delivering antigens and/or immune adjuvants for enhancing their presentation to the antigen-presenting cells thereby contributing to the efficient induction of the immune responses[28,29]. In drug discovery and development, the nanoparticles have been also considered as, screening tools at the drug discovery stage to identify molecules of significant therapeutic activity and those suitable for further development to human, as translational tools for understanding the biological mechanism of a disease or for validation of disease targets, and to develop added-value therapeutic versions of the patent expired drugs for life cycle management[1,30]. Thus, it is not exaggerating to mention that the nanoparticles are becoming integrated tools in discovery and development in pharmaceutical and biotechnology areas.

Additionally, the nanoparticles have been well demonstrated for use in diagnostic imaging, as magnetic resonance contrasts or as fluorescence agents, either *per se* or as carriers, to

track the nanoparticle biodistribution in the body or for detection of pathologies in the body. This is evident from a variety of products approved for commercialization for human application, based mainly on iron oxide[6], such as, Ferumoxsil, Ferumoxide, Ferrixan, Ferristene, and from those products in early stages of proof of concept for near-infrared fluorescence imaging, magnetic resonance imaging, positron emission tomography, ultrasound imaging, etc.[31,32]. Recently, considerable emphasis has been made about designing of the inorganic nanoparticles with renal clearance properties for use as contrast agents[33-35].

The concept of nanotheranostics[12,36,37], wherein the nanoparticle-based systems with combined capability of drug delivery and imaging, *i.e.*, addressing the drug to the target tissue/cell and simultaneously allowing the monitoring of response to the treatment, is emerging at a good pace in the context of personalized medicine.

The details of nanotechnology-based products commercialized for drug delivery and imaging has been provided in the table 1.

3. When nanoparticles encounter blood circulation

Following the exposure of the body to nanoparticles, be it through skin or by inhalation or by oral uptake or by injection, after the first point of contact, *i.e.*, skin membrane after skin exposure, the nasal epithelium, lung epithelium and the pulmonary cells after inhalation, the stomach and intestinal epithelia after oral uptake, and the blood following injection, the nanoparticles either distribute to the local tissues or are potentially transported to the systemic circulation and subsequently to the various tissues in the body. When nanoparticles enter into contact with blood, various interactions could be described within the nano-bio interaction space, as below.

3.1. Interaction with blood/plasma proteins:

The fundamentally important principle in the context of nanoparticles is the size and surface area relationship. The particle surface area and the size are inversely related, thus the surface area increases with decreasing particle size. Surface property of nanoparticles is another important factor influencing the nano-bio interactions. When the nanoparticles enter into contact with the blood circulation, the blood components, such as, plasma proteins and other biomolecules compete for binding onto the nanoparticle surface resulting in the formation of the nanoparticle-protein complexes with protein corona on the nanoparticles surface. Thus, the surface property of the nanoparticles before coming into contact with blood may turn out to be very different after their contact with blood. Depending on the affinity of blood/plasma proteins to the nanoparticle surface, the proteins may adsorb and desorb in a dynamic fashion leading to a corona, and at a given point of time, the protein corona may be either soft (containing reversibly binding proteins with faster exchange rate) or hard (containing irreversibly binding proteins with slower exchange rate)[38,39]. The kinetics of nanoparticle-protein association and dissociation process may have important roles in determining the particle's interactions with biological surfaces and the receptors and thus the nanoparticles overall fate[40]. Furthermore, the proteins adsorbed onto the nanoparticle surface may undergo conformational change and consequently may exhibit functional change[41]. The nanoparticles often curved and exhibiting high surface area may stimulate the proteins to adjust structurally to enable occupying the surface. For instance, binding to nanoparticles resulted in confirmation change of various proteins, such as, albumin[42], tubulin[43], transferrin[44], etc. Such undesired conformational changes in the protein structure may have important implications in terms of protein-protein interactions, cellular signaling and the related mechanisms. Thus, it is not surprising that the nanoparticles distributed to a tissue interact with the cells not with its original size and surface characteristics but with the newly acquired protein-corona induced size and surface characterisitics. It means that the nanoparticles interaction with the cells within a tissue is probably more mediated by the nature and confirmation of the surface bound proteins, and so as for the cellular internalization of the nanoparticles[45]. So, the key question here is what drives the nanoparticle-protein interactions. It is becoming clearer that the nanoparticles' physicochemical characterisitcs prior to contact with the biological milieu are those which regulate the biophysical properties. Mainly, the

nanoparticles' size and surface charge are the important decisive factors in differential protein adsorption and protein corona formation on the nanoparticles surface[46,47]. The plasma protein binding onto the nanoparticles of size as small as 80 nm diameter (6% protein bound) was shown to be lower compared to that of the nanoparticles of 240 nm diameter (34% protein bound)[48]. *In vivo*, the intravenously injected nanoparticles of diameters ranging between 80-150 nm underwent rapid systemic clearance with a plasma half-life of 8 – 30 min as compared to the small sized nanoparticles of 20 – 40 nm which exhibited a plasma half-life of 25 – 30 h[49,50].

On the other hand, the neutral charged nanoparticles experienced less protein adsorption compared to that of the negative and positive charged nanoparticles[51]. The nanoparticles size was also shown to influence the affinity of proteins to the particle surface and also the changes in protein structural conformation and function[52,53]. Moreover, the protein adsorption onto the nanoparticles was also influenced by the nanoparticles shape prior to contact with the proteins[54].

The biophysical properties of such nanoparticle-protein complexes *in vivo* influence the biodistribution of nanoparticles[55,56]. Adsorption of opsonins such as complement, fibrinogen, immunoglubulinG (IgG), etc. is believed to promote macrophage uptake and subsequent phagocytosis resulting in the nanoparticles clearance from the systemic circulation[57,58], whereas, binding of dysopsonins such as human serum albumin, apolipoproteins etc. regulate the nanoparticles distribution and accumulation in specific tissues[59]. Adsorption of apolipoproteins on the intravenously injected nanoparticles surface stimulate the interaction of nanoparticles with low density lipoprotein receptors, thus either promoting their transport across the blood-brain barrier[60] or their accumulation in the liver parenchyma[61], tissues which have abundance of lipoprotein receptors. This suggests the importance of understanding the nano-bio interactions, and making the link between the physicochemical characteristics of nanoparticles and their biophysical properties, to be able to anticipate the nanoparticles performance and safety.

3.2. Interaction with immune system components:

The nanoparticles encountering the blood stream also experience interaction with the components of the immune system, potentially resulting in the consequences, such as, the induction of complement activation, coagulation, and inflammatory response. Complement is one of the important components of the immune system which acts as a 'watch dog' against the

invading pathogens. Thus, the complement system acts as a first line of defense in the innate immunity and also play an important role in the induction and regulation of the adaptive immune B-cell and T-cell immune responses. Complement is a complex and large network of over 30 plasma and membrane proteins organized into a hierarchy of proteolytic cascades starting from the recognition of invading pathogens and the consequent steps of the immune activation[62]. Whatever the activation pathways suggested for the activation of complement, they all result in the production of a major complement fragment C3b. C3b possess the ability to induce opsonization and also results in the complement effectors, by the action of C3 convertases to result in the formation of membrane attack complex C5b-9, and by the action of C5 convertases to result in anaphylotoxins C3a, C4a and C5a which mediate inflammation. While complement function is crucial for the body's immunity, the uncontrolled/excess activation of complement is known to result in anaphylactic reactions and even to death[63]. Nanoparticles, due to their small size, extensive surface area, composition and functionality, possess great potential to interact with complement stimulating molecules and subsequently induce complement activation[64-66]. Moreover, nanoparticles possessing different surface charge exhibited different abilities to induce complement activation. For instance, the positively charged particles induced higher levels of complement activation compared to negatively charged and neutral charged particles[67].

Moreover, the complement effectors formed in response to complement activation are shown to directly enhance blood coagulation. Such effect is supported by the inflammatory mediators leading to the thrombogenicity of blood. For instance, the anaphylatoxin C3a activates platelets thereby, enhancing their aggregation and adhesion, while the anaphylotoxin C5a enhances blood thrombogenicity[68]. Complement and coagulation pathways activate each other, for instance, thrombin formed during the coagulation pathway and platelets are suggested to catalyse the amplification of complement. Complement was also reported to inhibit anticoagulant factors. In addition, the complement and coagulation are suggested to be the partners in inducing the inflammatory response[68].

The anaphylatoxins C3a and C5a formed during the complement pathway have been suggested also to contribute to the regulation of the inflammatory cytokine response and influence the production and secretion of tumor necrosis factor-α and interleukin-6[69,70].

Thus, the nanoparticles-mediated complement activation may be the cause of concern, as discussed above, due to the consequential undesired effects, such as, coagulation and mounting of inflammatory response linked to the stimulation of the secretion of cytokines and subsequent inflammatory mediators[71,72].

4. Pharmacokinetics and biodistribution of nanoparticles

4.1. Opsonization and nanoparticles clearance:

Whatever the route of exposure and absorption, once the nanoparticles reach the blood compartment, the nanoparticles are recognized by the immune system and thus are opsonized. This phenomenon is true for almost all types of nanoparticles, whether surface-modified or not, although the kinetics of the process may vary. Opsonization is a process of adsorption of plasma proteins onto the nanoparticles surface, making the particles prone to the processing by the immune system and/or modifies their biodistribution. Two types of opsonins, *i.e.*, immune and non-immune opsonins interact with the nanoparticles in the blood. The immune opsonins are those that recognize nanoparticles as foreign objects and direct those to the immune system (*i.e.*, to macrophages for phagocytosis), and comprise of complement proteins (different sub-classes of immunoglobulins, e.g. IgG, IgM), and complement-related proteins (e.g. C-reactive protein, serum amyloid protein, mannose-binding protein). The non-immune opsonins comprising of albumin, fibronectin, apolipoproteins, etc. are those that act as ligands and thus modify distribution of nanoparticles by interacting with specific receptors on the cell types[73].

The binding of opsonins onto the nanoparticles surface may be facilitated by one or various types of forces, such as, van der waals, electrostatic, hydrophilic/hydrophobic interactions[57]. Opsonin binding often determines the biodistribution and fate of the nanoparticles. The opsonized nanoparticles are recognized and captured by the resident macrophages of the organs of reticuloendothelial system (RES) (e.g. liver and spleen), and thereby the nanoparticles are cleared from the blood compartment and are accumulated in the RES organs. The nanoparticles capture by the macrophages occurs either by the recognition of the nanoparticle-bound opsonins by the specific phagocytic receptors expressed on macrophages or by the non-

specific adsorption process[57]. Such accumulation of the nanoparticles in the RES organs may be undesired or desired depending on the type of the intended application of nanoparticles. For instance, the passive accumulation of nanoparticles in liver tissue may be beneficial for delivering therapeutic substances or imaging agents to the liver parenchyma and hepatocytes, while the macrophage-mediated accumulation may be beneficial for delivering drugs to the macrophages for the treatment of macrophage-hosted diseases[74].

Nanoparticle clearance from the systemic circulation and from the tissues may also be impacted by the balance in the T-helper type 1 and type 2 (Th1 and Th2) cell responses exhibited by the T-lymphocytes. These responses lead to the secretion of different sets of cytokines and chemokines which possess the ability to polarize the macrophages to M1 or M2 phenotypes. Th1 responses induce polarization of macrophages to M1 phenotype possessing slower nanoparticle clearance property, whereas, the Th2 responses induce M2 phenotypic macrophages possessing rapid nanoparticle clearance property[75,76], because the M2 macrophages express higher levels of different scavenger and lectin receptors compared to M1 phenotypic macrophages. Thus, the immune status of the subject and its impact on the nanoparticle clearance should be taken into account for assessing the nanoparticles pharmacokinetics and distribution and for interpretation of the *in vivo* data.

Opsonization-mediated systemic clearance of the nanoparticles has been shown to be minimized considerably by surface coverage of the nanoparticles with hydrophilic polymers. Coating of the nanoparticles surface with hydrophilic non-ionic polymer poly(ethylene glycol) (PEG), has been widely demonstrated to minimize opsonization of the nanoparticles and thereby enhance their systemic longevity[77,78]. The chain length and density of PEG chains on the nanoparticles surface was shown to regulate the opsonin binding by steric repulsion of the proteins approaching the nanoparticles surface[79,80]. PEG molecular weights starting from 2 kDa are considered to be suitable to achieve the nanoparticles with prolonged systemic circulation time (also termed as 'long circulating nanoparticles')[81]. The concept of PEGylated long circulating nanoparticles was successfully developed which led to the commercialization of PEGylated liposomal doxorubicin (Doxil® / Caelyx®), while the docetaxel-loaded polymeric

nanoparticle formulation BIND-014 is currently in phase II clinical testing for oncology application.

PEG has been widely considered as an inert polymer with non-immunogenic nature. However, the immunogenic property of PEG and its ability to stimulate the induction of anti-PEG antibodies, and the influence of these antibodies on the clearance of subsequent doses (doses following first injection) of PEGylated liposomes[82], polymeric nanoparticles[83], conjugates[84] (generally termed as 'accelerated blood clearance' (ABC) phenomenon) compromizing the product efficacy has been the topic of frequent debate and controversy since several years. While the immunogenicity of PEG has been frequently demonstrated in various publications, both in animals and in humans[85,86], some recent studies have argued that a majority of the assays reported for anti-PEG antibodies may be flawed and lack specificity which urged the need of designing standard assays[87].

The hypothesized mechanism of ABC phenomenon of PEGylated particles involved the production of anti-PEG IgM in the spleen, in a T-cell independent manner by directly activating the marginal zone B-cells, and selective binding of anti-PEG IgM on to the PEG of subsequent doses of the PEGylated particles administered into the body[88]. In case of PEGylated liposomes, it was hypothesized that these antibodies lead to complement activation and resultant opsonisation of the subsequent doses of the PEG liposomes administered into the body and/or inducing leakage of the liposome leading to the release of the encapsulated payload[89]. Interestingly, however, it has been found that the physicochemical characteristics of PEGylated systems, and the time spacing between two administered doses, and the diameter of nanoparticles, influenced the ABC phenomenon. For instance, the methoxy-PEG in the formulation induced high levels of anti-PEG antibodies compared to the hydroxy-PEG[90], and the nanoparticles of smaller diameter induced lower levels of antibodies as compared to the bigger particles (70nm particles vs 120 nm particles), and maintaining a spacing of at least 2 weeks between two injections of PEGylated products resulted in overcoming the ABC phenomenon issue with the PEGylated nanoparticle products[91]. Thus, in light of the previous reports on PEG's potential immunogenicity, the impact of physicochemical charactersitics of PEG and PEGylated particles, and the time spacing between injections, the PEGylated nanoparticles should be appropriately characterized, and

detailed *in vitro* and *in vivo* assessment of the safety aspects of PEGylated nanoparticles should be considered.

4.2. Nanoparticles biodistribution driven majorly by their physicochemical characteristics:

The nanoparticles distribution in the body is highly dependent upon their physicochemical characteristics, such as, particle size and dispersity, surface charge, and surface functionality.

4.2.1. Impact of particle size and distribution:

The distribution of nanoparticles from systemic circulation to the tissue compartments is locally controlled by the type of vascular endothelium lining a specific tissue. Generally, the blood capillaries are of three types; the continuous, the fenestrated, and the discontinuous endothelium. Continuous endothelial vessels are found especially in lung, muscle, skin and nervous system, and fenestrated vessels (intercellular gaps of ≤ 100 nm) especially in kidneys, intestinal mucosa, synovial lining of bone joints, while the discontinuous vessels (intercellular gaps of > 100 nm) occur in liver, spleen and bone marrow[92]. The nanoparticles of size range up to 200 nm diameter undergo passive accumulation in the liver through the intercellular gaps, with particles of size < 100 nm diameter accumulating at high concentration due to the presence of higher density of intercellular gaps of this diameter compared to that of the the gaps of 200 nm[93,94]. In addition to such passive accumulation, active uptake of opsonized nanoparticles by liver-resident macrophages also results in the concentration of nanoparticles in liver. Although both passive and active mechanisms result in nanoparticles accumulation in liver, the compartments within the liver tissue in which the accumulation occurs may be different such that the actively accumulated nanoparticles concentrate in kupffer cells, whereas, the passively accumulated nanoparticles reach liver parenchyma and the hepatic cells, and thus the resultant impact on nanoparticles performace may be different. The nanoparticles of size bigger than 200 nm diameter are filtered in spleen[95], while those of sizes up to 60 nm diameter distribute into the bone marrow interstitial space and access the locoregional lymphatic drainages via the reticulo-endothelial cell-mediated phago-endocytic transfer[96].

The nanoparticles, if aggregate into bigger sized particles during the course of their circulation in blood, are then filtered mechanically by the pulmonary capillaries and thus are retained in the lung tissue. Thus, the size stability of nanoparticles is essential to minimize such accumulation, if at all it is undesired. The nanoparticles of sizes smaller than 10 nm diameter are filtered by the kidneys and are subsequently excreted from the body, while the particles bigger than 10 nm diameter distribute to the kidney tissue[97,98].

4.2.2. Impact of nanoparticles' surface charge:

Nanoparticles' surface charge also plays an important role both on the biodistribution of nanoparticles and also on the interaction with blood components. In the blood compartment, the positive charge on the surface of cationic nanoparticles facilitates non-specific electrostatic interaction with the blood cells potentially leading to hemolysis. The charged nanoparticles surfaces are shown to attract plasma proteins through electrostatic interaction, although the non-electrostatic interaction mediated protein binding also occurs. In the tissues, the positive charge favours the interaction with the negatively charged cell membranes. Such electrostatic interaction between the nanoparticles and cell membranes may be beneficial in cases where such interactions are intended, but in unintended cases; such interaction may result in non-specific toxicity resulting from the sticking of nanoparticles to the cells[99]. Alternatively, the nanoparticles exhibiting neutral surface charge show minimal interaction with the biological system compared to that of the charged nanoparticles[100]. The neutral nanoparticles showed slower opsonisation and thus lower RES uptake compared to negatively charged nanoparticles[101]. The uptake of nanoparticles by the tissues was also shown to be influenced by the nanoparticles surface charge. For instance, the nanoparticles uptake by the liver is increased by the strong negatively charged NPs[50]. In addition, the positively charged nanoparticles were shown to induce liver toxicity and dramatic proinflammatory response compared to the negatively charged and neutral nanoparticles[102]. Thus, prudent consideration of the surface charge of nanoparticles for a defined application, and the evaluation of its potential impact on the biophysical properties and subsequently on nanoparticles safety is essential.

4.2.3. Impact of nanoparticles shape/morphology:

The shape of nanoparticles has been also shown to have implications on nanoparticles pharmacokinetics and biodistribution. Nanoparticles' shape impacted their uptake by the macrophages, and consequently their systemic clearance. More importantly, the nanoparticle uptake by the macrophages depends on the orientation of nanoparticle at the point of contact with the macrophage. Thus, the geometry of interaction of nanoparticle and macrophage may either facilitate or inhibit the nanoparticle phagocytosis. For instance, if the nanoparticle is ellipsoidal or spiral, then the phagocytosis is efficient if it is presented from its tip portion to the macrophage rather than the major axis which exhibits high aspect ratio[103-105]. Spherical particles are readily phagocytosed by the macrophages due to the presence of high curvature regions in these particles, whereas, reducing the high curvature regions by elongating the particles with the same volume as that of the spherical particles, considerably inhibits their phagocytosis[102]. In this context, some types of non-spherical nanoparticles, even if they are not PEGylated, were shown to exhibit prolonged systemic circulation property[106,107].

Furthermore, using nanodiamond particles, it has been shown *in vitro* that the nanoparticles possessing sharp shapes such as those having sharp corners and edges, irrespective of the size, surface properties and composition, pierced through the endosomal membranes in the hepatic carcinoma cells and trafficked into the cytoplasm. These nanoparticles in turn showed prolonged cytoplasmic residence and thus a reduced elimination from the cells[108]. On the other hand, the cellular dynamics of spherical particles were different since they pierced less efficiently through the endosomal membrane and thus persisted inside the endosomes, and thus evolved with the endosomal maturation and subsequently eliminated rapidly from the cells via exocytosis[109].

Shape and morphology of nanoparticles has been also shown to dictate the nanoparticles biodistribution to tissues *in vivo* and their penetration within the tissue, following intravenous injection in tumor bearing mice. In fact, the spherical-shaped and disc-shaped nanoparticles exhibited significantly higher distribution to the tumor tissue as compared to that of the nanoparticles possessing rod-shape and cage-shaped, whereas, the rod-shaped and cage-shaped nanoparticles penetrated efficiently within the tumor tissue unlike that of the spherical-shaped

and disc-shaped particles which remained mainly at the tumor periphery[110]. Thus, the physicochemical characteristics of the nanoparticles responsible for their biophysical behaviour are crucial to understand and control, from the pharmacokinetic and biodistribution standpoint.

4.2.4. Impact of nanoparticles rigidity:

Rigidity is one of the characteristics of nanoparticles shown to influence their interaction with biological components and their behavior *in vivo*. Nanoparticles with low rigidity, and thus fluidic characteristic, may undergo deformation during their interactrion with biological system and thus may exhibit a different behavior compared to that of the rigid particles. For instance, Polyacrylamide particles of size ≥1000 nm produced with varying rigidity by altering the cross-linking density of the particles were shown to be taken up by macrophages at different intensities[111]. The particles with high rigidity (i.e. those prepared using high crosslinker concentrations) were taken up by macrophages more efficiently compared to that of the particles with low rigidity, although, these less rigid particles were able to adhere to the macrophages surface but were not efficiently phagocytosed. Rigidity was also suggested to influence the distribution of the injected liposomes of 200 nm diameter[112,113]. When injected in a mouse model, these liposomal particles exhibited higher distribution to liver parenchyma, although particles of such size cannot easily pass thorugh hepatic endothelial pores, suggesting particle deformation *in vivo* facilitating higher hepatic accumulation. Similarly, liposomal formulations with different membrane rigidities (prepared using different membrane rigidity modifiers) were shown to exhibit varying intensity of pharmacological effects due to the differences in the release kinetic of the encapsulated payload[114]. Thus, when administered intranasally into rabbits, liposomes with low rigidity and thus highly fluidic membrane characteristic[115] showed rapid leakage of the encapsulated protein insulin, and consequently led to high glucose reduction compared to that of the liposomes with high membrane rigidity which exhibited high stability and slow insulin leakage.

4.2.4. Impact of nanoparticles composition:

The composition of nanoparticles may also impact the nanoparticles' physicochemical properties, and in turn, their pharmacokinetics and biodistribution. The nature of composition, such as, type of lipid components, lipids with varying chain lengths, varying lipid content/concentrations, varying chain lengths of surface modifying polymers, etc., in a nanoparticle may have considerable impact on the nanoparticles' interaction in biological environment and their *in vivo* fate. For instance, the phospholipid-based liposomes composed of low and high concentrations of cholesterol (termed as 'cholesterol-poor' and 'cholesterol-rich', respectively) exhibited different interactions with serum proteins, resulting in differences in internalization by the liver macrophages and by the spleen macrophages *in vitro* in presence of serum[116]. The cholesterol-poor liposomes were taken up by liver macrophages in higher quantities compared to that of cholesterol-rich liposomes, whereas, opposite effect of uptake was observed by the spleen macrophages. This effect was suggested to be the result of differences in the extent of adsorption of opsonins onto cholesterol-poor and cholesterol-rich liposomes, and thus differences in interaction of these opsonin-bound liposomal types with the liver and spleen macrophages.

The length of acyl chains of PEG-lipids used in lipid nanoparticles composition influenced the kinetic of PEG desorption from the nanoparticle surface, and consequently, a different *in vivo* systemic clearance rates were found with nanoparticles containing PEG-lipids having different acyl chain lengths, when injected intravenously into mice[117]. The nanoparticles containing PEG-lipids with short C_{14} acyl chains showed a systemic half-life of 5-6h owing to a rapid desorption of PEG chains from the particle surface, whereas, the nanoparticles with long C_{20} acyl chains showed systemic half-life up to 10-12h due to a slow desorption of PEG chains from the nanoparticle surface, suggesting the impact of the nature of PEG-lipids on the pharmacokinetics of nanoparticles.

In case of polyethylene glycol-polylactic acid (mPEG-PLA) polymeric nanoparticles, alteration of the ratio of hydrophilic component PEG to the total mass of the copolymer in nanoparticles composition was shown to result in nanoparticles of different structures such as micelles or solid nanoparticle aggregates or vesicles[118]. Such differences in structural properties

may influence the nanoparticles *in vivo* behavior. For instance, when injected intravensouly in preclinical models, the mPEG-PLA nanoparticles made using polylactic acid of small molecular weight (2kDa) were found rapidly eliminated from blood circulation after few minutes of administration due to poor stability and subsequent degradation to PEG and PLA chains, whereas, the nanoparticles made from large molecular weight polylactic acid (30 kDa) were more stable and showed prolonged systemic circulation[119,81]. Additionally, it was shown that the polymeric nanoparticles compositions containing varying PEG content or PEG lengths showed different plasma protein adsorption profiles when incubated *in vitro* with plasma[80]. Nanoparticles with 5% PEG content adsorbed ~3-folds lower quantity of plasma proteins compared to that of nanoparticles with 2% PEG content, while variation in PEG lengths had resulted in differences in the types of proteins adsorbed onto the nanoparticles.

The nanoparticles compositions containing small quantities of residual stabilizers used for manufacture were shown to impact the nanoparticles interaction with the cells. For instance, the presence of residual stabilizer polyvinyl alcohol in PLGA nanoparticles composition was shown to negatively impact the cellular uptake of these nanoparticles *in vitro*[120]. Overall, the potential of the differences in nanoparticles composition on their interaction with biological milieu and thus their *in vivo* behavior should be taken into account during their biopharmaceutical assessment.

5. Nanoparticles toxicity assessment: *In vitro*

It is clear from that described in the previous section that the physicochemical characteristics of the nanoparticles, such as, size, surface characteristics and shape dictate their biophysical properties. The nanoparticles designed from different materials which exhibit varying chemical compositions and those designed from different processes potentially exhibit different physicochemical characteristics, and such differences may result in altered nano-bio interactions which may have different implications from performance and safety standpoint of the nanoparticles. Thus, for any new type of nanomaterial developed for biomedical application, a detailed understanding of the nano-bio interactions, toxicological properties, and the associated

mechanisms, using appropriate tools and methodologies is crucial for anticipation of its performance and safety.

Especially, the safety assessment of the nanoparticles should be performed using both *in vitro* and *in vivo* models. *In vitro* assessment has certain advantages over *in vivo* assessment, such as, low quantities of samples needed for testing, rapidity, lower cost, better control on variability, allows studying the mechanistic aspects, and minimizes the use of laboratory animals and sometimes minimizes sacrificing of the laboratory animals required for testing. The *in vitro* studies including mechanistic understanding of the nano-bio interactions, both at molecular and genetic level, undoubtedly serve during the interpretation of *in vivo* preclinical data and subsequently for the interpretation of the clinical data. Despite of the above advantages, the *in vitro* assays cannot be considered as a standalone or substitute to the *in vivo* assays which allow the real determination of the toxicity in the complex biological environment, because of the challenges associated with simulating *in vivo* conditions in *in vitro* models. Also, in *in vitro* conditions, the nanoparticles are in direct contact with the cells and thus remain as a reservoir at higher concentrations close to the cells, whereas, *in vivo* the nanoparticles distribute throughout the body and the fraction of nanoparticles reaching the cells may not be as dramatic as that happens *in vitro*. Thus, appropriate attention is needed during the interpretation of the *in vitro* toxicity results. In this section, the *in vitro* assays potentially useful for the assessment of nanoparticles toxicity, their principles, methodologies, benefits and challenges wherever relevant, have been described (see Figure 2).

The main components of the body which are exposed to nanoparticles, after any route of administration or exposure, are the blood components and the cells/tissues. Thus, the *in vitro* toxicity assessment is generally performed to understand the nanoparticle-biological interaction and safety at the cellular level and/or at the level of blood components.

5.1. Interaction with cells: This section provides details of the principle and methodology of various *in vitro* assays used for the toxicity assessment of nanoparticle systems.

5.1.1. Cellular morphology modification: It is one of the most important events that can be used for determining toxicity of nanoparticles to the cells. Changes in morphology of cells, such

as, change in shape, irregularity in shape, clump formation, shrinking effect, etc. compared to that of the untreated cells following treatment with nanoparticles could be visualized using phase contrast microscopy starting from 100X magnification or by using electron microscopy.

5.1.2. Cell proliferation assays:

5.1.2.1. Tetrazolium salts assay:

This assay involving the use of the tetrazolium salts, such as, MTS (3-(4,5-dimethylthiazol-2-yl)-5-(3carboxy methoxyphenyl)-2- (4-sulfophenyl)-2H-tetrazolium, inner salt) or MTT (3-(4, 5-dimethylthiazol-2- yl)-2, 5-diphenyltetrazolium bromide) which are reduced intracellularly by the living cells to produce formazan dyes (Figure 3) whose absorbance can be quantified using spectroscopy, is the most widely used assay for *in vitro* cell toxicity assessment. Mitochondrial succinate dehydrogenases of the living cells bioreduce the incubated soluble tetrazolium salts to the insoluble purple coloured formazan crystals which are impermeable to the cell membrane. These insoluble crystals accumulate within the healthy cells[121], which are then solubilized by the addition of solvents such as DMSO (Dimethyl sulfoxide) or detergents (e.g. sodium lauryl sulfate), and the absorbance of the resultant colour is measured using visible light spectrophotometer[122,123]. The percentage of surviving cells can be calculated as the absorbance ratio of the treated to the untreated cells.

The benefits of this assay compared to other toxicity assays include simplicity, faster, and the need of simple optical density acquisition[124], while the drawbacks include the inefficiency of some human cell lines at processing tetrazolium salts. Additionally, the changes in the pH of the culture medium, culture media supplements such as serum, cholesterol, ascorbate[125] etc. may alter the measurements and thus needs particular attention during interpretation of the assay results.

5.1.2.2. Alamar blue assay: This assay is a cell viability indicator which measures the reductive environment in the cell cytoplasm during cell metabolism, which is measured spectrophotometrically through the conversion of fluorimetric/colorimetric redox indicators. Upon incubation of the cells with alamar blue, the metabolic activity of cells reduces alamar blue

(resazurin, the oxidized form), a non-toxic, non-fluorescent, cell permeable product, to Resorufin (the reduced form), a bright red fluorescence product that can be measured at 590nm[126] (Figure 4) which reflects the viable cell number and changes in the cellular redox activity[127]. This assay was used to determine the cell viability of Cobalt-ferrite nanoparticles using normal mouse dendritic cells and also a variety of cancer cell lines[128].

The disadvantage of this assay is that it is not a direct cell counting technique, and sometimes a false change in fluorescence may result due to auto-reduction of resazurin. Alternatively, the auto-reduction can be inhibited by incorporating suitable redox stabilizing agents (eg. potassium ferrocyanide, ferric salt, ferricinium) in the control and the test samples. The unintended reduction of resorfin to dihydroresorfin which is a non-colored, non-fluorescent product may also occur resulting in the loss of the desired end point. The formation of dihydroresorfin can be inhibited by addition of poising agents such as methylene blue, toluidine blue, azure I and gallocyanide in the concetrations sufficient to maintain the potential of the growth medium above -0.1 volts[129].

5.1.2.3. [^{3}H]-thymidine incorporation into the newly synthesized cellular DNA: Uptake of [^{3}H]-thymidine into newly synthesized DNA during S-phase (synthesis phase) of the cell cycle is a sensitive measurement of the cell proliferation. Following treatment of cells with the nanoparticles whose toxicity is to be assessed, the cells are isolated and incubated with [^{3}H]-TdR. After pre-determined incubation time, the cells are washed to remove the un-incorporated label and the label incorporated into cellular DNA is measured using scintillation counter. The drawbacks associated with this method include the cost of the radioactive material, and also the need of special training and the approved facility to work with radioactive materials[130]. Moreover, the radioactive isotope ^{3}H in [^{3}H]-TdR was shown to inhibit to a certain extent the rate of DNA synthesis thereby potentially interfering with the assessment, and thus the use of non-radioactive stable isotopes instead of radioactive isotope has been suggested[131].

5.1.2.4. Clonogenic assay: Clonogenic assay, also termed as colony forming efficiency (CFE) assay, can be used to study the impact of the nanoparticle samples on the cell survival and proliferation over extended periods of time (up to several weeks). The methodology involves

incubation of cells with nanoparticles sample whose impact on the cells is to be assessed, followed by staining of the cells with crystal violet or nuclear stains, and counting the colonies of the proliferating cells by visual observation[132]. This method has been successfully employed for the assessment of the effects of carbon nanotubes on human bronchial epithelial and on human keratinocyte cell lines[133]. Interestingly, it was observed that increasing doses of the nanotubes resulted in decreased number of colonies, suggesting a dose-dependent toxicity of the nanotubes *in vitro*.

5.1.3. Necrotic assays: Necrosis is a form of injury and/or unprogrammed premature cell death. Necrosis commonly occurs when the cells encounter extreme physiological conditions, such as, hypothermia, hypoxia etc., resulting in the damage of the cell membrane and subsequently the release of cytoplasmic contents including lysosomal enzymes into the extracellular environment. *In vivo,* the necrotic cell death is often associated with tissue damage resulting in an intense inflammatory response. Necrosis can be assessed by verifying the cell membrane integrity by using dyes, such as, Trypan blue[134], Propidium iodide[135], Neutral red[136], and also by assessing the enzymatic activity such as lactate dehydrogenase (LDH) [137].

5.1.3.1. Trypan blue assay : Trypan blue assay is based on the principle that the live cells possess intact cell membrane which excludes the trypan blue, a negatively charged dye, whereas, the dead cells are permeable to the dye and thus take up the dye to result in a strong absorbance at 605 nm. In this assay, the cell suspension pre-treated with nanoparticle sample whose impact is to be assessed is incubated with TB, and is then visually examined using microscopy to determine whether the cells take up or exclude the dye. Viable cells appear not colored as these cells do not take up the dye, whereas, dead cells take up the dye into the cytoplasm and thus appear blue in colour[138]. The number of viable cells, an increase or decrease, in comparison to the untreated cells is counted and the ratio determined. The advantages of this assay include simplicity and low cost, while the drawbacks include potential variability associated with the cell counting apparatus such as hemocytometer[139], and also that even the living cells take up the dye if incubated with the dye for longer durations. For instance, TB assay has been reported for the

assessment of cytotoxicity of the nanocrystalline magnesium ferrites ($MgFe_2O_4$) of about 20 nm diameter on the MCF-7 breast cancer cell line[140].

5.1.3.2. Propidium iodide assay: Propidium iodide is a negatively charged DNA intercalating fluorescent agent employed to analyze the cell cycle events using flow cytometric measurements of cellular DNA. Propidium iodide does not permeate through the viable cell membranes and thus is excluded by the viable cells. In the permeable cells, propidium iodide binds to and intercalates with DNA and RNA thereby staining these nucleic acids whose content could be measured using flow cytometry. Thus, for specific DNA analysis, the samples are treated with ribonuclease to eliminate RNA. The methodology involves incubation of the cells with the nanoparticles samples whose toxicity assessment is intended. After the predetermined interval, the cells are washed with pH 7.4 phosphate buffered saline (PBS). About 1 x 10^6 cells are incubated overnight at 4°C in 70% ethanol to fix and permeabilize the cells, and subsequently centrifuged to remove ethanol, washed with PBS, and treated with extraction buffer (a mixture of 192 parts of 0.2M disodium hydrogen phosphate and 8 parts of 0.1M citric acid). Then the cells are washed with PBS and treated with deoxyribonuclease-free ribonuclease-A (200µg/ml) for 30min at 37 ^{0}C to inactivate RNA to be able to measure DNA. Then the cells are stained with propidium iodide (50µg/ml) in PBS for about 10 min followed by the measurement using a flow cytometer[141]. Quantification of the cellular DNA content using this assay provides information such as the identification of the cells in various phases cell cycle phases, the DNA damage, and the measurement of the apoptotic cells.

5.1.3.3. Neutral red assay: The principle of neutral red assay is that the viable cells take up the neutral red dye (3-amino-7-dimethylamino-2-methylphenazine hydrochloride), which is unionized at physiological pH, by active transport and incorporate into the intracellular lysosomes where the dye gets protonated (Figure 5) and thus accumulate, while the dead cells do not take up the dye. The methodology involves the incubation of cell suspension post-treatment with the nanoparticles samples whose toxicity testing is intended, with the neutral red dye for 2 to 4 h, and subsequently washing the cells in PBS followed by extraction and spectrophotometric quantification of the incorporated dye. This assay is cost-effective and more sensitive than other

cytotoxicity assays such as tetrazolium salts assay[142], while the potential drawback is the impact on the dye quantification results by the agents that affect the lysosomes within the cells where the dye is retained.

5.1.3.4. Calcein acetoxymethyl ester / ethidium homodimer assay: This assay involving the labeling of living cells is based on the principle of the enzymatic conversion of virtually non-fluorescent cell-permeable calcein violet acetoxymethylester (obtained by the modification of anionic carboxylic acid functions of calcein violet with the acetoxymethylester groups) to the intensely fluorescent anionic calcein violet (λex at 400 nm and λem at 452 nm) by the intracellular esterases by hydrolysis in the living cells[143,144] (Figure 6). Intracellular esterases cleave the parent compound to the anionic fluorescent dye calcein violet which is retained in the cells to a much greater extent than its uncharged parent compound. The methodology involves the incubation of cell suspension treated with the nanoparticles samples whose toxicity assessment is intended, with the calcein violet acetoxymethylester solution (whose stock solution is prepared in anhydrous dimethylsulfoxide to avoid hydrolysis of the compound) for about 30 minutes. The cells are centrifuged, washed once with PBS, and are observed either using fluorescence microscope or are analyzed using flow cytometer.

Ethidium homodimer (EthD-1) (5,5'-[1,2-ethanediylbis(imino-3,1-propanediyl)]bis(3,8-diamino-6-phenyl) dichloride dihydrochloride) is a high-affinity nucleic acid stain which exhibits 40-folds enhancement in the fluorescence after binding to the cellular DNA (λex at 528 nm /λem at 617 nm)[145] (Figure 7). When incubated with the cell suspension, EthD-1 enters the cells with damaged membranes and exhibit enhanced bright red fluorescence that could be visualized using fluorescent microscope or by flow cytometer, but is excluded by the living cells with intact membrane.

A combined assay to determine both the living and the dead cell population in the cell suspension following treatment with the nanoparticles samples whose toxicity assessment is intended could be carried out by incubating the cell suspension with both calcein violet acetoxymethylester which allows the measurement of living cell population and Ethidium homodimer which allows the measurement of the dead cell population. This assay could be

carried out using Live/Dead® viability/cytotoxicity kit (Molecular probes, Invitrogen technologies)[146].

5.1.3.5. Lactate dehydrogenase (LDH) assay: This assay could be used to assess the cell membrane damage by determining the cytoplasmic LDH release into the medium following incubation with the nanoparticles sample whose toxicity assessment is intended or to assess the cell viability by lysing the membrane of the living cells using the detergent Triton X100 and subsequently quantifying the total LDH levels. LDH is a stable cytoplasmic oxido-reductase enzyme that catalyzes the inter-conversion of pyruvate to lactate in the living cells (Figure 8A). LDH catalyzes the reduction of nicotinamide adenine dinucleotide (NAD^+) to NADH, which is subsequently used to stoichiometrically convert the INT ((2-(4-Iodophenyl)-3-(4-nitrophenyl)-5-phenyl-2H-tetrazolium chloride)) to a red colored soluble formazan product (Figure 8B) whose absorbance can be measured spectrophotometrically at 490 nm wave length. For example, the LDH assay was used to assess the toxicity of silver, molybdenum and aluminium nanoparticles possessing diameters ranging between 15 to 30 nm[147]. The nanoparticles-treated cells showed considerable LDH leakage suggesting plasma membrane damage and thus the nanoparticles-induced cell toxicity.

5.1.4. Apoptotic assays: Apoptosis is a programmed cell death characterized by cell shrinkage, cell membrane blebbing, formation of giant cells, nuclear breakdown, micronucleus formation, DNA fragmentation, etc. (Figure 9). Apoptosis is considered vital for various biological processes, whereas, the uncontrolled apoptosis may lead to undesired consequences. Apoptosis of the cells may be assessed by microscopic examination and by using a variety of assays, such as, Annexin-V assay, DNA laddering assay, Caspase assay, Comet assay, TUNEL assay, etc.

5.1.4.1. Annexin V-FITC/Propidium iodide assay: Phosphatidyl serine, a phospholipid, which is typically oriented toward the cytoplasmic side of the cell membrane of healthy cells, becomes exposed to the outer side of the cell membrane in the cells undergoing apoptosis[148]. Thus, the expression of phosphatidyl serine on the cell membrane is considered as one of the hallmarks of

the cellular apoptosis. Annexin V, a calcium dependent phospholipid-binding protein possesses a high affinity for phosphatidylserine, and is employed in the form of conjugate with the fluorescent probe fluorescein isothiocyanate (FITC) for the determination of the presence of phosphatidylserine moieties on the cell membrane of apoptotic cells. Annexin V-FITC bound onto the apoptotic cells can be detected by fluorescence detection and can be quantitatively measured using flow cytometry.

A combination assay wherein the cells are treated with Annexin V-FITC and propidium iodide allows the differentiation among the early apoptotic cells which are annexin V positive and propidium iodide negative, the late apoptotic cells which are annexin V positive and propidium iodide positive, and the viable cells which are negative to both annexin V and propidium iodide. For instance, the Annexin V-FITC/propidium iodide assay was employed to determine the *in vitro* toxicity and induction of apoptosis by silica nanoparticles possessing 20 nm diameter on human HepG2 hepatoma cells and normal human L-02 hepatic cell lines[149]. The results revealed a dose-dependent induction of apoptosis by the nanoparticles, and the assay allowed distinguishing the early and the late phase apoptosis in the cells.

5.1.4.2. Microscopic assessment of apoptotic bodies: The morphological characteristics of the apoptotic cells, such as, condensation and marginalization of chromatin, fragmentation of nuclei, cell shrinkage can be identified by staining the cells with Hoechst stain (e.g. Hoechst 33258). The methodology involves treatment of the nanoparticles-treated cells fixed and placed on the glass slides with Hoechst stain dissolved in citric acid [0.01 M], disodium phosphate [0.45 M] buffer containing 0.05% Tween-20, followed by observation of the cells under fluorescent microscope[150] and counting various apoptotic bodies to calculate their percentage and comparison with the control cells (*i.e.* the cells not treated with nanoparticles sample).

5.1.4.3. DNA laddering/ DNA fragmentation assay: DNA fragmentation, the cleavage of chromatin DNA into 180-200bp oligonucleosomal units, is a hallmark of apoptosis[151]. When run on gel electrophoresis, the cleaved oligomers appear as a DNA ladder. In the cells undergoing apoptosis, caspase-3 (the member of cysteine-aspartic acid protease family) initiates the DNA fragmentation by proteolytic inactivation of the Inhibitor of caspase activated deoxyribonuclease

(ICAD), resulting in the release of the endonuclease, *i.e.*, caspase activated deoxyribonuclease (CAD) that causes DNA fragmentation[152]. The assay methodology involves subjecting the cells treated with nanoparticles whose toxicity assessment is to be done, to the DNA extraction and isolation, followed by resolving the isolated DNA on 1.5% agarose gel containing 3 µg/ml ethidium bromide and subsequently visualizing the bands using a UV transilluminator[153]. Alternatively, the cells could be lysed using the DNA fragmentation lysis buffer (0.1% Triton X-100, 5 mM Tris-HCl, pH 8.0, 20 mM EDTA), followed by the selective precipitation of the unfragmented, high-molecular weight DNA using polyethylene glycol 8000, while the fragmented DNA remaining in the supernatant can be directly analysed using agarose gel electrophoresis or using the fluorescent dye Hoechst 33258[154].

For instance, silver nanoparticles when incubated with HT-1080 Human fibrosarcoma and A431 Human skin carcinoma cells induced apoptosis as observed from the oligonucleosomal DNA fragments or DNA laddering at the nanoparticles concentration of 6.25 µg/ml indicating the nanoparticles toxicity, as assessed using the DNA laddering assay[153].

5.1.4.4. Comet assay or single cell gel electrophoresis: DNA damage in the cells, if any, resulting from the exposure to nanoparticles could be determined using comet assay. In this assay, the cells pre-incubated with nanoparticles sample whose toxicity assessment is intended, are lysed to remove proteins and the DNA is denatured under alkaline or neutral conditions, stained with ethidium bromide and subjected to electrophoresis to observe the broken DNA fragments or damaged DNA portions. The degree of DNA damage is detected by the extent of tailing (appear as a comet). Using this assay, the kinetics of the progression of DNA fragmentation could also be elaborated[155]. The main drawback of comet assay includes its inability to measure fixed mutations.

5.1.4.5. TUNEL (Terminal deoxynucleotidyl Transferase mediated dUTP-biotin Nick End Labeling) assay:

During apoptosis, the chromatin structure of the cellular DNA is degraded into fragments of 50-300 kilobases and small oligomers of about 200bp with a large number of 3^1-OH ends exposed. The TUNEL assay relies on the ability of the enzyme terminal deoxynucleotidyl transferase, an

exogeneous DNA polymerase-I which repairs isolated DNA fragments, to incorporate the fluorochrome labeled dUTP (e.g. Br-dUTP) into free 3'-hydroxyl termini generated by the fragmentation of genomic DNA into the low molecular weight double-stranded DNA and the high molecular weight single stranded DNA[156]. The DNA analysis could be carried out either using flow cytometry or by image analysis.

TUNEL assay has been employed for the evaluation of the toxicity of metal oxide nanoparticles, such as, copper oxide (CuO) and silica (SiO_2) on human adenocarcinoma A549 cell line[157]. When the cells were incubated with these nanoparticles at the concentrations of 30µg/ ml for 8h, no significant differences between the control and the nanoparticles-treated cells were observed suggesting the lack of toxicity by the nanoparticles at the concentration tested.

5.1.4.6. Assay of mitochondria-dependent apoptosis: Involvement of mitochondria in apoptosis could be assessed by examining various aspects, importantly the measurement of the overexpression of Bax and Cytochrome-C, and the caspase-3 cleavage analysis.

Bax, an important pro-apoptotic protein of the Bcl-2 family, can trasclocate to the outer mitochondrial membrane and insert into the mitochondria and forms oligomers contributing to the formation of mitochondrial permeability transition pore (PTP). Opening of the mitochondrial PTP can lead to the release of Cytochrome C which is a key indicator of the mitochondrial dependent apoptosis pathway. Methodologically, the cells are incubated with nanoparticles for pre-determined time interval, followed by harvesting about $1x10^7$ cells. The proteins Bax and Cyt-C are then extracted from the cells using protein extraction kit and are subsequently quantified using BCA protein assay kit. Protein samples are then resolved using sodium dodecyl sulfate-polyacrylamide gel electrophoresis (SDS-PAGE) and are subsequently transferred onto the nitrocellulose membranes. The membranes are washed, incubated with anti-Bax antibody and anti-cytochrome-C antibody at 4^0C overnight. Immunodetection is then performed with secondary HRP-conjugated antibody[158].

5.1.4.7. Caspase-3 assay

Caspases (Cysteine-requiring Aspartate proteases) are a family of proteases which are important entities in the process of apoptosis. Caspase-3 is a member of CED-3 (Caenorhabditis elegans gene ced-3) subfamily of caspases and is one of the critical enzymes of apoptosis. It can process procaspases and specifically cleave most of the caspase-related substrates including many key proteins involved in apoptosis regulation[159] leading to cell death. In addition, caspase-3 plays an important role in mediating nuclear apoptosis including chromatin condensation, DNA fragmentation and cell blebbing[160]. The activity of caspase-3, if elevated in the cells as a result of nanoparticles treatment, can be determined using caspase-3/CPP32 colorimetric assay kit. This assay is based on the hydrolysis of the peptide substrate Asp-Glu-Val-Asp p-nitroanilide (DEVD-pNA) by casapse-3, leading to the release of p-nitroaniline which is assessed spectrophotometrically at 405 nm.

5.1.5. Assays for understanding the mechanism of toxicity

5.1.5.1. Measurement of ROS: Nanoparticles toxicity may disturb the oxidative balance of the cell resulting in the production of abnormally elevated concentrations of ROS[161] (e.g. superoxide anion (O_2^-), free radicals (e.g. hydroxyl radical ($OH^\cdot$), peroxy radical ($ROO^\cdot$) and hydrogen peroxide (H_2O_2)) or reactive nitrogen species (RNS) (e.g. nitric oxide ($NO^\cdot$), peroxynitrite ion ($ONOO^-$), peroxy nitrous acid (ONOOH)). ROS and RNS exhibit toxic effects by damaging the DNA, proteins and lipids in the cells resulting in the abnormal cellular function. The cellular ROS could be measured using various methods differing in specificity, sensitivity, and the ability to measure intracellular and/or extracellular ROS.

5.1.5.1.1. DCFH (2,7-Dichlorodihydrofluorescein) assay: In this assay, 2,7-dichlorofluorescein diacetate (DCFH-DA), a non fluorescent probe, is used in which the diacetate moiety provides lipophilicity to the molecule and thus its cell penetrating ability. Intracellularly, DCFH-DA is hydrolyzed by esterases to the impermeable non-fluorescent reduced DCFH (2^1,7^1-dichlorofluorescein) which is rapidly oxidized by the intracellular ROS to highly fluorescent 2^1,7^1-dichlorofluorescein (DCF) (Figure 10). The fluorescence of the resultant DCF could be measured at λ_{ex} of 485 nm and λ_{em} 520 nm[162], wherein the measured fluorescence intensity is proportional to the ROS levels in the cytoplasm.

Briefly, the methodology involves the incubation of nanoparticles-treated cells with DCFH-DA solution (methanolic solution of DCFH-DA diluted in serum- and additive-free culture medium) at 37°C for 30 min. The cells are then washed with PBS to remove excess DCFH-DA, lysed in alkaline solution, followed by centrifugation for 10 min. The fluorescence intensity of DCF formed in the supernatant is measured at λ_{ex} of 488 nm and λ_{em} of 525 nm[163,164].

5.1.5.1.2. EPR (Electroparamagnetic resonance) technique: EPR spectroscopy has been widely used for the assessment of nanoparticle induced ROS generation. It allows the identification and quantification of specific free radical generated by using specific spin traps or probes. For instance, the probe 5,5-dimethyl-1-pyrroline-N-oxide (DMPO) which is specific for the formation of hydroxyl radical (DMPO reacts with the hydroxyl radicals and forms DMPO-OH)[165] or 1-hydroxy-4-phosphonooxy-2,2,6,6-tetramethylpiperidine (PP-H) specific for the formation of superoxide anion[166] are incubated with the cells treated with the nanoparticles whose toxicity assessment is intended, and the supernatant is isolated and analyzed using EPR spectrophotometer[167,165]. This method has been successfully employed for the cytotoxicity assessment of titanium dioxide nanoparticles of 100 nm size on human bronchial epithelial cells[168].

5.1.5.1.3. Plasmid DNA scission assay: This assay has been used to assess ROS production in some studies[169,170] by using circular bacterial plasmid DNA that is wound into supercoiled structure. Presence of ROS particularly hydroxyl radicals, cleave the bonds holding the supercoiled structure, thereby the circular structure becomes unwind and may sometimes to linear in the presence of high ROS content. These various forms of DNA could be distinguished by their electrophoretic mobility on agarose gel wherein the mobility of supercoiled structure is higher that that for the circular form. Ethidium bromide staining of the gel allows the quantification of the supercoiled band intensity and its depletion is a measure of plasmid damage by the ROS[171]. This is not generally considered as a sensitive technique since some fractions of DNA may bind to the nanoparticle surface.

5.1.5.1.4. Oxidative stress assays: Oxidative stress is defined as the excess formation or inefficient removal of highly reactive species due to the imbalance created between pro-oxidants (eg: ROS) and anti-oxidant defense mechanisms of the body[172]. The oxidative stress markers include superoxide dismutase (SOD), catalase, Glutathione, Glutathione reductase, Glutathione transferase, and Lipid peroxidation. Of these, superoxide dismutase is an importance antioxidant enzyme which catalyses the dismutation of superoxide anion ($O_2^{\cdot -}$) into H_2O_2 and molecular oxygen (O_2) providing an important defense against the oxidative damage. The levels of oxidative stress markers, in case of toxicity, may be either elevated or depleted[173-175,163].

5.1.5.1.4.1. Measurement of Superoxide dismutase activity: Various assays, such as, Xanthine-xanthine oxidase assay (XOD) and Nitroblue tetrazolium (NBT) assay have been employed for the measurement of SOD activity indirectly[176]. SOD activity in the experimental samples is measured as the percentage inhibition of the rate of formation of formazan dye. In xanthine-xanthine oxidase assay, the superoxide anions generated as a result of the conversion of xanthine and O_2 to uric acid and H_2O_2 reduce the tetrazolium salt WST-1 into WST-1 formazan dye whose absorbance is measured at 450 nm. Addition of the test sample (nanoparticles-treated) containing SOD to this reaction reduces superoxide anion levels, thereby lowering the rate of formation of formazan dye indicated by a decreased absorbance at 450 nm, which is a measure of the activity of SOD in the test sample. This method possesses drawbacks, such as, the poor water solubility of formazan dye and its reaction with the reduced form of xanthine oxidase.

In Nitroblue tetrazolium assay, the superoxide anions generated during autooxidation of the added hydroxylamine reagent, convert the water-soluble yellow coloured NBT to the blue coloured NBT-diformazan which can be measured spectrophotometrically at 560 nm. Presence of SOD in the test sample reduces the superoxide anion levels by converting it to H_2O_2 and molecular oxygen thereby lowering the rate of formation of diformazan dye.

5.1.5.1.4.2. Measurement of Catalase activity: Catalase is another important antioxidant enzyme that catalyzes the decomposition of hydrogen peroxide into water and oxygen molecules[177]. The presence of catalase (increased or decreased levels) in the test sample can be assessed by the addition of hydrogen peroxide. The methodology involves mixing of the cell

lysate obtained from the cells treated with nanoparticles, containing known amount of protein, with potassium phosphate buffer (pH 7.0) containing H_2O_2. The decrease in the absorbance of H_2O_2 is measured spectrophotometrically at 240 nm. Catalase activity is calculated from the slope of the H_2O_2 absorbance curve and normalized to the protein concentration[178].

Catalase also exhibits peroxidase activity, in which low molecular weight alcohols such as methanol serve as electron donors. This assay is based on the principle that the enzyme catalyzes the conversion of methanol, in the presence of H_2O_2, to formaldehyde which then reacts with chromogenic substrate, 4-amino-3-hydrazino-5-mercapto-1,2,4-triazole (called as purpald) resulting in the formation of a colourless compound (Figure 11). This compound upon oxidation forms a purple coloured product which can be spectrophotometrically measured.

5.1.5.1.4.3. Measurement of Glutathione (GSH) activity: GSH is an antioxidant present in the cells, whose functional role is to detoxify the ROS and hence essential in maintaining the reduced environment in the cells.

$$\mathbf{R\bullet + GSH \rightarrow RH + GS\bullet}$$
$$\mathbf{GS\bullet + GS^- \rightarrow GSSG\bullet^-}$$
$$\mathbf{GSSG\bullet^- + O_2 \rightarrow GSSG + O_2\bullet^-}$$

At high concentrations of ROS exposure, an imbalance between the levels of oxidized glutathione (GSSG) and reduced glutathione (GSH) is observed. Such changes in GSH: GSSG ratio is an indicator of oxidative stress which can be assessed using liquid chromatographic methods[179]. Appropriate care should be excercised when using this method because during chromatographic estimation process, autooxidation may potentially occur leading to the overestimation of GSSG.

One of the frequently used methods to measure GSH is the O-phthaldialdehyde (OPA) method. OPA is non-fluorescent and reacts with sulfahydril and primary amino groups of GSH to result in the formation of highly fluorescent iso-indole adducts (OPA-GSH adducts) (Figure 12A).

GSH can also be measured by using DTNB (5,5-dithio-bis(2-nitro benzoic acid), Ellman's reagent)[180] in presence of NADH which facilitaes the reduction of GSSG to GSH by glutathione reductase. The sulfahydril group of GSH subsequently reacts with DTNB resulting in the formation of yellow colored 5-thio-2-nitro benzoic acid (TNB) ((Figure 12B) which can be measured colorimetrically at 412 nm to obtain the concentration of GSH.

5.1.5.1.4.4. Measurement of Glutathione peroxidase (GPx) activity: Glutathione peroxidase is an antioxidant enzyme which catalyses the detoxification of H_2O_2 and lipid hydroperoxides by GSH[181] thereby protecting the cells against oxidative damage.

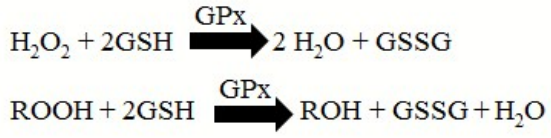

Glutathione peroxidase activity can be assessed using lipid hydroperoxide substrate tertiary-butyl hydroperoxide[182]. In this method, the presence of GPx in the cell lysate catalyses the detoxification of t-butyl hydroperoxide by GSH (reduced form) resulting in the formation of GSSG (the oxidized glutathione) which is subsequently recycled to GSH by glutathione reductase in the presence of NADPH present in the reaction mixture.

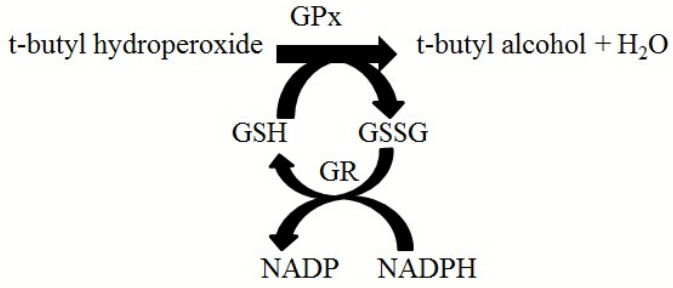

The methodology involves the addition of reaction mixture containing t-butyl hydroperoxide (30 mM), reduced GSH (2 mM), GPx (0.5 unit/ml) and NADPH (0.25 mM) to the cell lysate, followed by measuring the decrease in NADPH absorbance for 3 min spectrophotometrically at 340 nm. GPx activity is calculated from the NADPH absorbance standard curve.

5.1.5.1.4.5. Measurement of Glutathione reductase (GR) activity: Glutathione reductase catalyses the recycling of GSH from GSSG in presence of NADPH, thus offering protection against the oxidative stress. GR activity is measured by the addition of the reaction mixture containing 0.1 M phosphate buffer (pH 7.4), 0.66 mM GSSG and 0.1 mM NADPH to the cell lysate, and any decrease in NADPH absorbance can be measured spectrophotometrically at 340 nm. GR activity is calculated from the NADPH absorbance standard curve[183].

5.1.5.1.4.6. Measurement of Glutathione-s-transferases (GSTs) activity: Glutathione transferases are antioxidant enzymes which catalyze the conjugation of electrophilic substrates to GSH, and thus are involved in the detoxification process[184]. GST activity is assessed from its ability to mediate the conjugation of GSH with CDNB (1-chloro-2,4-dinitrobenzene), wherein the extent of conjugation leads to proportional change in the absorbance measured at 340 nm. The methodology involves the addition of the reaction mixure containing 1 mM GSH, 1 mM CDNB and 0.1M potassium phosphate (pH 6.5) to the cell lysate, followed by the measurement of absorbance spectrophotometrically at 340 nm[185].

5.1.5.1.4.7. Measurement of Lipid peroxidation (LPO): LPO is defined as the oxidative deterioration of lipids containing C=C bonds. LPO causes modification in the permeability and fluidity of membranes of mitochondria and lysosomes resulting in damage to these membranes. In case nanoparticles induce the oxidative stress in cells, the polyunsaturated fatty acids in the cellular lipid membrane may undergo peroxidation resulting in the formation of unstable lipid hydroperoxides which subsequently decompose into lipid peroxidation products, such as, Malondialdehyde (MDA), 4-hydroxynoneal (4-HNE). In presence of 2-thiobarbutyric acid (TBA), MDA reacts and leads to the formation of a red colored 1:2 MDA:TBA adduct which can be quantified colorimetrically to assess the extent of lipid peroxidation (Figure 13).

The methdology involves the incubation of 200 µl of cell suspension with 800 µl of reaction mixture containing TBA (0.4% w/v), SDS (0.5% w/v) and acetic acid (5% v/v, pH 3.5) for 1 h at 95°C. The sample is cooled and centrifuged at 5000 rpm for 5 min, and the absorbance of the supernatant is measured at 532 nm. The result is expressed as nM of MDA per mg of protein[163]. The drawback of this assay is that TBA is not completely specific for MDA, and

moreover the other types of compounds, such as, non-lipid-related materials as well as fatty peroxide-derived decomposition products also react with TBA[186].

5.1.6. Genotoxicity: Genotoxicity is a process of damage of cellular DNA by a chemical/agent resulting in the gene mutations. The unique physico-chemical characteristics of nanomaterials, such as, small size, extensive surface area, shape and composition enable the entry of nanomaterial into the cells and subsequently facilitate their interaction with the cellular components including the nucleus and the nuclear components to potentially alter the cell signaling and function resulting in genotoxicity. The genotoxicity may be of two types; primary genotoxicity and secondary genotoxicity. Primary genotoxicity, resulting from DNA damage induced by direct interaction of chemical/agent with nuclear DNA. Secondary genotoxicity is the toxicity mediated by the adverse effects, such as, inflammation, and oxidative stress in the cells[172]. Genotoxic assays are classified based on the evaluation of DNA strand breaks (using comet assay, see section 5.1.4.4), the assessment of chromosomal damage (using chromosomal aberration and cytokinesis blocked micronucleus assays), the identification of DNA base modifications (8-oHdG detection by ELISA), the determination of gene mutations (using Ames assay) and the alterations in gene expression.

5.1.6.1. Assessment of chromosomal damage: In addition to identifying mutations of a particular gene, it is also important to analyze the presence of chromosomal aberrations, such as, chromosome breaks, fusions and abnormal segregation and also the presence of micronuclei.

5.1.6.1.1. Chromosomal aberration analysis: This assay uses fluorescent *in situ* hybridization (FISH) to detect small deletions and duplications in the chromosomes which are not visible in microscopic analyses. FISH uses fluorescent probes such as small DNA strands that are complementary to specific parts of a chromosome and thus hybridize those, the hybridization could be visualized under fluorescence microscopy. Briefly, the methodology involves the incubation of cells with the nanoparticles for a pre-determined period and then allowed to grow in fresh medium for 24 h. Cells are then arrested in metaphase by the addition of colcemid

solution, and then subjected to hypotonic treatment with warm 0.075 M KCl and subsequently fixed with fixative (3:1 methanol:acetic acid solution). Metaphase spreads are prepared and FISH is then performed using telomere- and centromere-specific peptide nucleic acid (PNA) probes labeled with Cy(cyanine)-3 and FITC, and analyzed using the imaging system[187].

5.1.6.1.2. Cytokinesis blocked micronucleus assay (CBMN): CBMN assay measures the chromosomal breakage occurring as a result of nanoparticles toxicity to the cells. Micronuclei are small nuclei formed from chromosomal fragments or whole chromosomes which failed to incorporate into one of the daughter cells after cell division. The CBMN assay measures the chromosomal breakage occurring as a result of nanoparticles toxicity, if any, to the cells. Formation of micronucleus could be examined under fluorescent microscope. Using FISH technique with specific probes targeted to centromere region, it is also possible to determine whether a fragment of chromosome (Clastogenic event) or an entire chromosome (aneugenic effect) forms micronucleus. The major advantage of micronucleus assay is that it can detect both chromosomal and genetic mutations, whereas, the limitation of this assay is that it can be applied only to the dividing cells[172]. Micronucleus formation can be visualized using the dye H33258, a membrane permeable fluorescent DNA stain that intercalate in A-T rich regions of the DNA. Following incubation with the nanoparticles, the cells are washed with PBS and fixed overnight with fixative containing acetic acid-methanol (1:3 v/v). Cells are then washed and fixed on slides and stained with H-33258 (10 µg/ml). Slides are examined under fluorescent microscope to count the number of binucleated cells containing micronuclei and to calculate the fraction of cells containing micronuclei.

5.1.6.1.3. Identification of DNA base modifications: 8-hydroxyl-2'-deoxyguanosine (8-OHdG) detection using the enzyme linked immunosorbent assay (ELISA) technique: 8-OHdG, an indicator of oxidative damage of DNA, is a modified DNA base with a hydroxyl group at eigth position of guanine, and can be quantitatively detected by ELISA technique. The methodology of this assay[188] is schematized below and the chemical reaction scheme is shown in Figure 14.

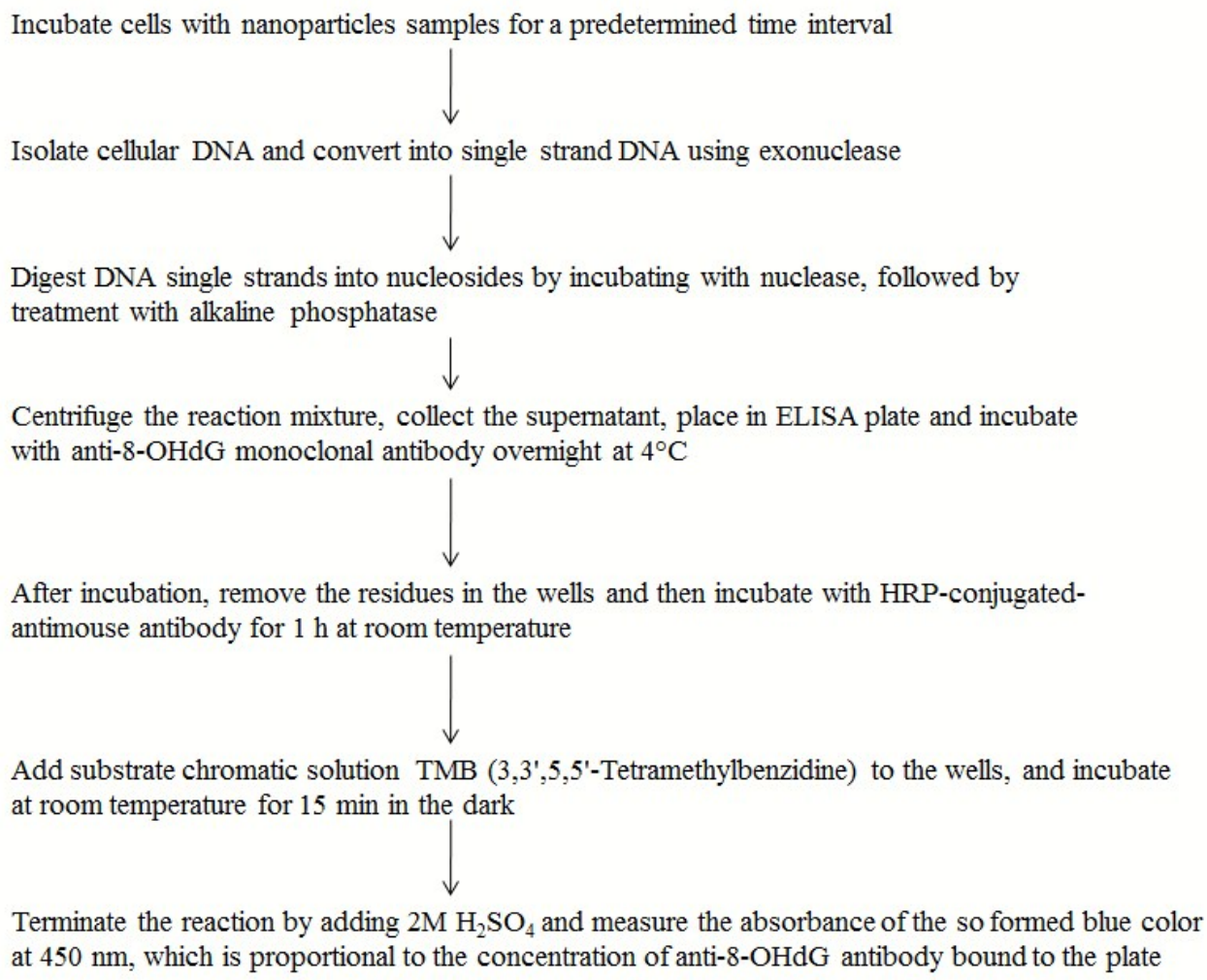

5.1.6.1.4. Identification of gene mutations using Ames assay: This assay has been used to determine the mutagenecity of a variety of nanomaterials, which employs the bacteria lacking DNA repair mechanisms and require histidine for their growth (e.g. Salmonella typhimurium)[189]. Following exposure to the nanoparticles whose genotoxicity is to be assessed, if the bacteria form colonies in histidine-free media, it indicates the reversion of bacterial phenotype to a histidine-positive phenotype due to a reverse mutation in the histidine locus. The methodology involves the incubation of overnight cultures of S.typhimurium strains with the nanoparticles whose genotoxicity is to be assessed, and are then mixed with sterile top agar containing 0.6% agar and 0.5% NaCl containing histidine- biotin, subsequently poured onto minimal glucose agar plates and then incubated at 37°C for 48 h. The revertant colonies are counted and the result is

considered positive for genotoxicity if the count of reverting colonies comes out to be double compared to that of the negative control[190]. However, this assay employs bacteria and not mammalian cells, and thus the results should be interpreted with caution. In any case, the Ames assay alone is not sufficient to assess genotoxicity, and thus other genotoxicity assays should be performed in addition to this assay.

Of various assays described above for the assessment of the genotoxicity, the most commonly used *in vitro* genotoxicity assays are the comet assay and the micronucleus assay[191].

5.1.6.1.5. Assays for alterations in gene expression:

Gene expression is a process by which the genetic information present in the gene is used in the synthesis of protein(s) required for cell growth and functioning. Gene expression profiling is a simultaneous measurement of the expression level of thousands of genes (particularly mRNA transcripts) to assess cell functioning. It discriminates between the cells that show active cell division or the cellular response following treatment with nanoparticles. Gene expression assays include Northern blot analysis, Ribonuclease protection assays (RPA), Quantitative real-time polymerase chain reaction (qRT-PCR), and microarrays[132].

5.1.6.1.5.1. Northern blot analysis : It is considered as a powerful method to measure the levels of mRNA in a quantitative manner, and also provides information about the size and sequence of mRNA molecules. RNA isolation is performed from nanoparticle-treated cells, separated on denaturing agarose gel containing 0.8 mol/l formaldehyde, and is then transferred onto nitrocellulose membrane. RNA on the membrane is hybridized to a radio-labeled RNA probe that is complementary to the target sequence. Membranes are then washed initially with 2X sodium chloride-sodium citrate solution and 0.1% SDS and then with 0.1 X SSC and 0.1% SDS. The hybridized RNA-radiolabelled probe is then detected by autoradiograph analysis[192]. The main drawback of this method is the need to use radioactive agents making the procedure time consuming and complicated to handle.

5.1.6.1.5.2. Ribonuclease protection assay: It is a sensitive method that simultaneously detects, quantifies and maps several RNA species. Following RNA isolation from nanoparticle treated

cells, the target RNA sequence is hybridized with labelled antisense probes. Unhybridized probes and RNA sample are then removed by digestion with a mixture of nucleases. Nucleases are then inactivated, samples are digested with proteinase-K and extracted with phenol-chloroform mixture. Following ethanol precipitation with 4M ammonium acetate solution, the hybridized samples are separated on Tris-borate-EDTA-urea gel, and subsequebtly analyzed using autoradiograph analysis[193]. The main limitations of this assay are that this assay does not provide information about the transcript size, and the lack of probe flexibility.

5.1.6.1.5.3. Quantitative real-time polymerase chain reaction (qRT-PCR) or real time reverse transcription followed by polymerase chain reaction : It is one of the sensitive methods for the quantitative measurement of mRNA. This method uses dyes such as SYBR Green (which emit fluorescence signal by binding to double stranded DNA), TaqMan (generates fluorescence depend on Forster resonance energy transfer-FRET by coupling of TaqMan and quencher to oligonucleotide substrates[194]. Following total RNA isolation from nanoparticle-treated cells, it is converted to single stranded cDNA (complementary DNA) in the presence of reverse transcriptase and oligo primers. Using this single stranded cDNA as a template, cDNA is amplified to double stranded DNA in the presence of specific primers and SYBR green dye[195]. The fluorescence signal generated from the dye is proportional to the amount of double stranded DNA present in the sample, from which the level of expression of mRNA of the target gene can be determined.

5.1.6.1.5.4. Microarray: Microarray technology involves the hybridization of nucleic acid target sequence to a large set of oligonucleotide probes, for the determination of gene sequence or for the detection of variations in gene expression. Microarray technology aids in simultaneous examination of the expression of thousands of genes in a single RNA. In this technique, mRNA molecules from nanoparticle-treated cells are isolated and converted to cDNA by RT-PCR using fluorescent dyes. The fluorescent labelled cDNA is placed on microarray slide containing synthetic complementary DNAs, where cDNA hybridizes to it and generate fluorescence. Bright fluorescence indicates overexpression of genes and lighter fluorescence indicates lower expression of genes. Thus, using this assay, the gene expression pattern, *i.e.*, the types of genes upregulated and the types of genes downregulated in the cells due to nanoparticle-treatment can

be analyzed. For instance, the incubation of mouse hepatic cells with poly(ethylene glycol)-block-polylactide nanoparticles, resulted in the over-expression of various ATP-binding cassette transporters and down-regulation of Glutathione-s-transferase P1 as assessed using mouse cDNA microarray and validated by RT-PCR assays[196].

5.2. Interaction with blood components:

Nanoparticles, either injected parenterally into the body, or after exposure through the local routes (e.g. oral, skin, eye), come into contact with blood and thus with various blood components including blood cells and plasma proteins. Due to their unique physicochemical characteristics, the nanoparticles possess great potential to interact with various blood components, and such interaction needs be well characterized and assessed from toxicological standpoint. Interaction of nanoparticles with blood components may be assessed for their compatibility with blood cells by the assessment of hemolytic potential and any alteration in hematological parameters, potential to stimulate the immune system including complement system, blood coagulation and inflammatory responses. Additionally, the assessment of nanoparticle-plasma protein interactions may also be considered to aid in nanoparticles toxicological assessment.

5.2.1. Hemocompatibility / Hemolysis :

Nanoparticles exposed to systemic circulation should be hemocompatible, whereas, undesired interaction with RBC may result in hemolysis and with other blood cells may induce the risk of modification of hematological parameters.

Hemolysis is a damage caused to the red blood cells leading to the leakage of hemoglobin into the blood. *In vitro* evaluation of the hemocompatibility of nanomaterials becomes an important part of *in vitro* characterization assays during their early preclinical development. Dobrovolskaia and colleagues[197] at National Characterization Laboratory USA has validated *in vitro* assay protocol for the determination of hemolytic properties of the nanoparticles. In this

assay, the nanoparticles are incubated with blood, and the hemoglobin released by the red blood cells following the damage caused by the nanoparticles is oxidized to methemoglobin by ferricyanide in presence of bicarbonate, and subsequently methemoglobin is converted to cyanmethemoglobin in presence of cyanide (Drabkin's reagent). The undamaged red blood cells in the blood sample are removed by centrifugation, and then the cyanmethemoglobin formed in the supernatant is measured spectrophotometrically at 540 nm (Figure 15). The hemolytic potential is assessed by comparing the resultant absorbance of the nanoparticle-treated samples with that of the control blood sample, using standard curve prepared using hemoglobin standards. According to ASTM (American Society for Testing and Materials Designation, Standard practice for Assessment of Hemolytic Properties of Materials Designation F-756-00), <2% hemolysis is considered to be non-hemolytic; 2-5% is considered slightly hemolytic; >5% is considered hemolytic. Percent hemolysis of the samples is calculated using the formula below:

$$\text{Hemolysis (\%)} = \frac{\text{Plasma free hemoglobin}^{*}\ \text{(mg/ml)}}{\text{Total hemoglobin present in whole blood (mg/ml)}} \times 100$$

* Free hemoglobin released into plasma due to hemolysis

In addition to assessment of hemolytic potential, the hemocompatibility of the nanoaprticles could be assessed by performing whole blood cell count including erythrocytes, leucocytes, thrombocytes (platelets), and verifying the differences, if any, in the blood cell count in the nanoparticles-treated blood samples in comparison to that of the untreated blood samples.

5.2.2. Complement activation:

In vitro assessment of the potential of nanoparticles to induce the activation of complement system is crucial because the activation of complement system, which is the first-line of innate immune defense system, *in vivo* may result in life-threatening hypersensitivity reactions[198]. Nanoparticle-induced complement activation may be assessed either by measuring the total functional complement level in plasma or serum employing the assay of hemolytic activity on sensitized sheep red blood cells[199], or by measuring the complement products / scission products employing specific ELISA assays[200]. The scission products include SC5b-9 (S-protein-bound form of the terminal complex generated by assembly of C5 through C9 by either classical or alternative pathways, which is a measure of C5a formation), Bb (proteolytically active fragment of factor B, a key marker of complement activation through alternative pathway), anaphylotoxins, etc. For instance, Szebeni[201] reported ELISA method for the assessment of complement activation (by measuring SC5b9) by liposomes by incubating with human serum in microtiter plate at 37°C under shaking. SC5b9 present in the particle-treated samples bind to monoclonal antibody already coated in the wells of microtiter plate resulting in the formation of SC5b9 complex, which is detected using HRP-conjugated antibodies. To the wells is then added 3,3',5',5' tetramethyl- benzidine substrate solution, and as a result, the wells containing SC5b9 complex-HRP conjugated antibody exhibits change in colour measurable spectrophotometrically at 450 nm. Alternatively, Hamad and colleagues[202] recently reported methodology for simultaneously testing various complement activation products Bb, C4d, C5a and SC5b-9 using ELISA. Methodologically, the assay is performed by placing 100 μL of fresh undiluted human serum (nanoparticle-treated or not) on the gels incubated at 37 °C, followed by withdrawing the serum samples at pre-determined intervals for the measurement of complement activation products. Zymosan served as a positive control for complement activation, while aggregated human immunoglobulinG served as positive control for activation of complement by classical pathway.

5.2.3. Interaction with coagulation system:

Blood coagulation refers to the process of formation of clot to prevent bleeding. Platelets play an important role in clot formation together with clotting factors. These factors activated in a cascade manner results in the formation of fibrinogen, a soluble plasma protein, cleaved by thrombin into an insoluble protein fibrin. The fibrin proteins sticks together to form a clot. Interaction of nanoparticles with platelets and clotting factors in blood may result in undesired shift of hemostatic balance due to disturbance of the coagulation system[190] leading to the formation of disseminated clots in the vascular system.

The thrombogenecity of nanoparticles may be assessed by measuring their potential to induce platelet aggregation and modify the coagulation time[203]. Platelet aggregation assay involves the incubation of nanoparticles sample with platelet rich plasma (PRP) obtained from the freshly derived whole human blood. After 15 min of incubation, the PRP is analyzed using particle count and size analyser to determine the number of active platelets. The percent platelet count is calculated using the formula below, and the percent platelet aggregation above 20% indicates that nanoparticles are thrombogenic.

$$\text{Platelet count (\%)} = \frac{\text{Platelet count in negative control} - \text{Platelet count in test sample}}{\text{Platelet count in negative control}} \text{ x100}$$

The plasma coagulation time can be assessed by exposing the platelet-poor plasma from whole human blood, followed by analysis of prothrombin, activated partial thromboplastin time, and thrombin time[204,205]. Briefly, one volume of nanoparticles as aqueous suspension at defined concentrations is incubated with nine volumes of platelet-poor plasma at 37°C, and the coagulation can be assessed using coagulometer[204]. Additionally, the the effects of nanoparticles on plasma clotting factors can be assessed by diluting the test nanoparticle suspension in plasma with the plasma deficient in the factor the impact on which to be measured, and then comparing the clotting time with that of normal plasma[204]. For instance, using this assay, the effect of non-PEGylated poly(lactic acid) and PEGylated poly(lactic acid) nanoparticles on plasma clotting time and on clotting factors has been assessed. Interestingly, non-PEGylated nanoparticles prolonged considerably the clotting time and have also reduced slightly the levels of factors VIII,

IX, VII and X but decreased factor V level by 20-30%, whereas, PEGylated nanoparticles did not show any eefect on coagulation time and on clotting factors[204], thus suggesting the importance of PEG in minimizing the interaction of nanoparticles with coagulation system.

5.2.4. Inflammatory response:

It is a protective response offered by the tissues to injury. Due to complex interactions of multiple cell types, measurement of inflammatory response *in vitro* is challenging, while the pro-inflammatory substances responsible for inducing the inflammatory response can be quantified. The most commonly measured pro-inflammatory markers include cytokines and/or chemokines, using ELISA method. The cytokines and chemokines linked to inflammatory response include Tumor necrosis factor- α, Interleukin-8, Interleukin 1-α, Interleukin 1-β, Interleukin -6, Granulocyte macrophage colony stimulating factor. Assesment of the pro-inflammatory markers in the cells suspension or body fluids post-treatment with nanoparticles samples is performed using the pro-inflammatory marker-specific ELISA kits[206-208].

5.2.5. Plasma protein binding onto nanoparticles surfaces :

As described in the previous sections, when nanoparticles encounter blood circulation, the plasma proteins are adsorbed onto the nanoparticle surface resulting in the formation of dynamic protein corona. The biophysical properties of such nanoparticle-protein complexes *in vivo* influences the nanoparticles biodistribution[55,56,73] and also lead to unwanted biological effects[209,210]. Thus, analysis of the protein corona formation on nanoparticles surface and the nature of corona is expected to provide important information about potential biodistribution and toxicity of the nanoparticles. Such approach may also aid in an integrated nanoparticle design wherein the nanoparticles of appropriate physicochemical characteristics could be designed by taking into account their intended biophysical properties.

Methodologically[38], the plasma protein corona on nanoparticles can be analyzed by incubating the nanoparticles samples with plasma in 10 mM phosphate, 0.15 M NaCl, 1 mM EDTA for 1 h. The samples are centrifuged to recover the nanoparticle-protein complexes.

Proteins are eluted from nanoparticles by adding SDS-sample buffer, and the eluted proteins are then separated on 12% SDS- PAGE one dimensional gel. Bands of interest from the gels are eluted and digested with trypsin resulting in the formation of peptide mixtures which are subsequently resuspended in 0.1% formic acid and analyzed using liquid chromatography mass spectrometry to determine the qualitative and quantitative composition of the protein corona. These proteins are classified based on their physicochemical and biological properties using relevant bioinformatic tools[211]. Alternatively, techniques such as Protein Lab-on-Chip® and capillary electrophoresis have been also reported for the assessment of serum protein adsorption onto nanoparticles surfaces[212]. The Protein Lab-on-Chip® allowed the determination of kinetics of protein adsorption onto the nanoparticles surfaces.

6. Nanoparticles toxicity assessment : *In vivo*

6.1. Key considerations

In vivo assessment of the toxicity of nanoparticles is crucial to understand their behaviour in the complex biological environment and to anticipate their safety in the intended species, animal or human. Additionally, the information on the metabolization potential of nanoparticles in the extracellular environment, the environment which the nanoparticles encounter before coming into contact with the cells, could be possible with *in vivo* assays but may be very challenging with *in vitro* assays. The *in vivo* assessment should include appropriate assays to understand the pharmacokinetics and biodistribution of nanoparticles, and their effects at the blood and the tissue level in short-term and long-term after administration of single and multiple doses relevant to the intended route of administration and application. Such assays are expected to provide information on the dose-dependent accumulation in desired and in undesired tissues, the concentration within the tissues, and the residence time in the tissues, based on which one can go back to the bench to understand *in vitro* the mechanism of their degradation and/or toxicity in corresponding cell type and at corresponding concentrations to assess the acceptability level of toxicity and anticipate the tolerable doses *in vivo*. Additionally, assessment of kinetics of degradation/metabolism of nanoparticles in the body allows defining the frequency of administration of nanoparticles product to the patients.

The biodistribution studies become further important when nanoparticles are associated with a therapeutic agent, for instance for drug delivery purposes. The safety of nanoparticle-associated therapeutic agent mainly depends on its affinity to the nanoparticle and on the nanoparticle biodistribution. If the nanoparticles distribute to the undesired compartments in the body and reside in these compartments for longer time, then safety is a measure of not only the nanoparticle carrier but also of the effects caused by therapeutic agent, especially if the agent is cytotoxic or its target lies in these compartments, at the site of prolonged residence. For instance, in case of polyethylene glycol-coated liposomal doxorubicin, one of the safety concerns in the patients treated with this product is the hand-foot syndrome (also called as 'palmar-plantar erythrodysesthesia')[213] resulting from extravasation of the drug-containing small liposomes into skin layers and subsequent release of the cytotoxic drug doxorubicin in the local tissue, leading to tissue irritation and inflammation[214]. Thus, the rate of clearance or degradation kinetics of nanoparticles in the accumulated tissues determines the local safety of nanoparticles in these tissues[215]. In addition, the metabolites emerging from nanoparticle degradation, in case toxic, may also be responsible for inducing local tissue toxicity. Thus, the *in vivo* assays of toxicity assessment should include all possible means of understanding the nanoparticles fate and its impact on the complex biological system, to de-risk its subsequent development chain toward the intended use.

Attention is also needed with respect to the interpretation of pharmacokinetic/biodistribution data. It is known that prolonged systemic circulation of the nanoparticles could be achieved by coating their surface with hydrophilic polymers such as polyethylene glycol due to its ability to mask the nanoparticle surface from recognition by the body's immune system and consequently limit their uptake by macrophages. However, the nanoparticles not coated with PEG may also exhibit prolonged systemic circulation at doses exceeding the phagocytic capacity of the macrophages, owing to the macrophage saturation, which may induce complications related to the blockade of macrophages' essential functions including increased risk of infections in the body[216]. Similarly, in case of macrophage saturation effect, the nanoparticles may not exhibit linear pharmacokinetics with dose, because of the depletion of macrophage uptake capacity at increasing nanoparticles doses due to saturation effect. Such effect may have implications on the predictability of the dose response and

pharmacokinetic data extrapolation. Thus, understanding of the macrophage saturation potential and in turn the recovery of macrophage activity *in vivo* following systemic exposure of the nanoparticles is critical to anticipate the potential hazards, and also to allow designing of injection schedule with time spacing between two doses appropriate to avoid macrophage saturation and the associated undesired effects.

With nanoparticles-based products, two types of variability in performances may emerge, such as, the variability linked to the nanoparticles physicochemical attributes, and the variability linked to the patient pathophysiology. While it is crucial to ensure reproducibility of the physicochemical attributes of nanoparticles formulations from chemistry, manufacturing and controls (CMC) standpoint in all manufacturing lots, taking into account the potential variability associated with patient pathophysiology is of equal importance as early as from preclinical development by design of relevant animal models for the proof of concept evaluation. For instance, the distribution of nanoparticles to healthy tissues may be considerably different from their distribution to the same tissues but in a pathological state, such as, inflammatory condition, compromised tissue endothelial wall, etc., while variations in other tissue-related parameters such as enzymatic composition, pH, etc. may have impact on the nanoparticle degradation kinetic and the release of encapsulated payload from nanoparticles. Thus, a prudent choice of *in vivo* models having pathophysiology closer to that of the target species for which the product is to be developed, be it for human or for animal, and the target indication in these species. Moreover, development of appropriate biopharmaceutical modeling approaches may allow better predictability of nanoparticle product performances and increase the probability of translation of preclinical proof-of-concept to clinic.

6.2. Assays

6.2.1. Blood compatibility and potential to induce acute hypersensitivity reactions

In a majority of the cases, the methodologies of the *in vitro* toxicity assays could be applied for the *in vivo* assessment after collection of blood or tissue samples from the animals. For instance, hematology parameters assessment allows assessing any damage caused to the blood cells

including red blood cells (erythrocytopenia/hemolysis), white blood cells and platelets (platelet aggregation/thrombocytopenia)[217]. Immune-related assays including the assay of markers indicators of the activation of complement system (e.g. complement activation products, plasma thromboxane B2 levels)[218] cogulation[204], inflammatory response (proinflammatory markers)[219] provide information on immune compatibility of the nanoparticles, while direct assessment of the effects resulting from immune activation, such as, hemodynamic changes[220], complement activation-related pulmonary hypertension, hypotension, etc. suggest acute hypersensitivity reactions[63].

6.2.2. Serum biochemistry parameters to detect indicators of organ toxicity

Serum biochemistry assay allows analysis of any changes caused by nanoparticles occurred in the serum biochemical parameters[217], mainly proteins (e.g. albumin, globulin), levels of liver enzymes (e.g. alanine aminotransferase, aspartate aminotransferase, alkaline phosphatase, gamma glutamyltransferase) and bilirubin indicators of liver tissue damage or dysfunction, levels of substances such as urea (blood urea nitrogen) and creatinine indicating kidney and/or hepatic dysfunction, levels of pancreatic enzymes (e.g amylase, lipase) indicators of damage to pancreas, creatine kinase indicator of muscle inflammation, levels of minerals such as calcium and phosphorus as indicators of toxicity to pancreas, kidney, etc., and other serum composition such as glucose, cholesterol and electrolytes.

6.2.3. Organ/tissue histology studies

Histopathology assessment using Hematoxylin Eosin and Saffran staining[221,222] and immunohistochemistry technique[223] allows determination of any undesired changes at the tissue level suggestive of the tissue toxicity of nanoparticles. Methodologically, organ/tissue histology is performed by isolation of tissue and placing it in melted paraffin overnight, followed by making tissue-embedded paraffin blocks. The blocks are cut into thin sections with thickness in the range of 1 to 5 µm, and these sections are placed on glass slides for treatment with toluene and ethanol sveral times to dehydrate and once finally with purified water to clean up the

solvents. These sections are then stained with Hematoxylin Eosin and Saffran dyes by successive washings with water or ethanol and finally with toluene, and then the sections are mounted for microscopic observation[141].

Genotoxicity assay *in vivo* could be performed by isolating cells from *in vivo* compartments, such as, bone marrow[224,225] and subsequent determination of micronucleus induction by microscopy, DNA damage and gene mutations using immunofluorescence detection.

6.2.4. Sub-acute, acute and chronic toxicity assessment

The toxicity assays should include also sub-acute, acute and chronic toxicity assessment after single dose and after multiple/repeated doses with various time spacing between the doses to understand the spatio-temporal accumulation and clearance of nanoparticles from various tissues and the related toxicity. The main parameters assessed, but not restricted to, include body weight, physical observations for limbs paralysis, fatigue, food intake, blood count, serum biochemistry, blood compatibility, complement activation, coagulation, inflammatory response, organ morphology and histology[226]. The major challenge is the development of relevant *in vivo* models allowing predict/anticipate the toxicity of nanoparticles intended for development to human use. Additionally, there is a need to develop appropriate mathematical modeling approaches to model the distribution and toxicity data collected from *in vitro* and *in vivo* studies, and taking into account the physiology and physiological differences within various body compartments, between different animal species, and between animals and humans[227], to predict/anticipate the toxicity risks in humans. This may allow for an appropriate design of the clinical studies using nanoparticles (e.g. selection of suitable dose regimens, protocols and biomarkers) and minimize the unknown toxicity-related surprises in the clinical trials.

7. Physiological based modeling of nanoparticles

Physiologically based modeling is extensively in pharmaceutical development, for the prediction of pharmacokinetic parameters of drug formulations in humans from data obtained in preclinical models and across various preclinical species, based on the integration of anatomical, physiological and biochemical aspects of the body and segmenting various organs into individual compartments and interconnecting those with the mass transportation and ADME properties of drugs[228]. Application of the classical physiology based modeling, generally used for drug development, to nanoparticles may not be straightforward because of the complexity associated with the interplay between nanoparticles' physicochemical characteristics and biophysical properties, distribution, metabolism, etc. Design of modeling approaches suitable for nanoparticles could be built on existing classical modeling experience, by taking into account additional nanoparticle-specific factors, such as, clearance by macrophages of RES organs and other mechanisms, differential extravasation through vascular endothelia of varying fenestrae dimensions, distribution influenced by plasma protein adsorption, cellular uptake and the associated kinetics and mechanisms, biodegradation, and elimination kinetics, etc.

For instance, MacCalman and coworkers[229] reported a model to describe body distribution of nanoparticles after administration by inhalation to rat. In this report, the distribution of inhaled nanoparticles from lungs to major organs of the body, such as, liver, kidney, spleen, heart, brain and gastrointestinal tract has been modeled, wherein various regions within lung are considered as different compartments and integrating into the model the translocation of particles to blood vessles and their subsequent distribution to other organs. Noteworthy, the model fit was found good for the total particle mass measured in the body and to the particle mass measured in some organs, such as, lung, brain, spleen but not for organs such as liver and kidney. Moreover, the optimal parameter estimates for model have been suggested to be dependent on nanoparticles' physicochemical characteristics and also on the routes of nanoparticles exposure to lung. Similarly, a model for describing the pulmonary retention and clearance of inhaled silica crystals in rat (median diameters of the order of 1.7 μm) and responses to dose, such as, inflammatory response and fibrosis has been reported[230]. Some studies have also reported attempts to build models to define relationship between the properties of

nanoparticles and their biodistribution[231-233], wherein model with appropriate fit simulating the experimental biodistribution data of nanoparticle formulations with varying characteristics has been described by Li and coworkers[233]. On the other hand, a model describing the simulation of time-dependent tissue distribution kinetics of quantum dot nanoparticles upto a period of 6 months after intravenous injection to mice has been also reported[234], wherein the prediction of tissue distribution kinetics by this model was consistent with the experimental data.

Overall, designing of relevant modeling approaches allowing prediction of performance and potential toxicities of new nanomaterials based on their material properties and physicochemical characteristics, although challenging, could be of high value for the design and development of nanoparticles with desired biopharmaceutical performance and safety, and also in regulatory perspective.

8. Conclusion

Nanoparticles, owing to their unique physicochemical characteristics, possess great potential to interact with the biological components, such as, blood, plasma proteins, tissues, cells and sub-cellular components. Those designed from new materials with varying architectures and functionalities aimed at enhancing the performance may potentially exhibit varying physicochemical characteristics and thus may have varying impact on the nanoparticles' biopharmaceutical properties. Thus, delineating the interplay between the physicochemistry and biophysical properties of nanoparticles, and their impact on the pharmacokinetics (absorption, distribution, metabolism and excretion), and toxicological properties, could be expected to allow designing of appropriate nanoparticles products for biomedical applications to human or veterinary use. The development of physiologically-based computational models allowing prediction of ADME properties and toxicity from the material and physicochemical characteristics may help in anticipating potential safety issues, and thus likely pave way toward the design of nanoparticles with desired biopharmaceutical performance and safety. More importantly, a thorough toxicological assessment *in vitro* with mechanistic details is considered

useful in anticipating the potential *in vivo* toxicity, and hence is expected to be valuable for extrapolation of preclinical data to human during the nanoparticles development.

Disclaimer

The views expressed by the authors in this review do not necessarily reflect the opinions of Sanofi.

References

1. D. V. Bazile, *J. Drug Del. Sci. Tech.*, 2014, 24, 12.
2. M. Johannsen, U. Gneveckow, B. Thiesen, K. Taymoorian, C. H. Cho, N. Waldöfner, R. Scholz, A. Jordan, S. A. Loening and P. Wust, *Eur. Urol.*, 2007, 52, 1653.
3. M. Johannsen, B. Thiesen, P. Wust and A. Jordan, *Int. J. Hyperthermia*, 2010, 26, 790.
4. E. A. Neuwelt, P. Várallyay, A. G. Bagó, L. L. Muldoon, G. Nesbit and R. Nixon, *Neuropathol. Appl. Neurobiol.*, 2004, 30, 456.
5. S. R. Digumarthy, D. V. Sahani and S. Saini, *Cancer Imaging*, 2005, 5, 20.
6. L. H. Reddy, J. L. Arias, J. Nicolas and P. Couvreur, *Chem. Rev.* 2012, 112, 5818.
7. K. K. L. Phua, H. F. Staats, K. W. Leong and S. K. Nair, *Sci. Reports*, 2014, 4, 5128.
8. N. Kamaly, Z. Xiao, P. M. Valencia, A. F. Radovic-Moreno and O. C. Farokhzad, *Chem. Soc. Rev*., 2012, 41, 2971.
9. M. Johannsen, B. Thiesen, P. Wust and A. Jordan, *Int. J. Hyperthermia*., 2010, 26, 790.
10. H. S. Huang and J. F. Hainfeld, *Int. J. Nanomedicine*, 2013, 8, 2521.
11. F. Liu, S. Laurent, H. Fattahi, L. Vander Elst and R. N. Muller, *Nanomedicine (Lond).*, 2011, 6, 519.
12. J. L. Arias, L. H. Reddy, M. Othman, B. Gillet, D. Desmaële, F. Zouhiri, F. Dosio, R. Gref and P. Couvreur, *ACS Nano*, 2011, 5, 1513.
13. J. Xie, S. Lee and X. Chen, *Adv. Drug Del. Rev.*, 2010, 62, 1064.
14. T. Dvir, B. P. Timko, D. S. Kohane, R. Langer, *Nature Nanotechnol.*, 2011, 6, 13.
15. L. M. Graham, T. M. Nguyen and S. B. Lee, *Nanomedicine*, 2011, 6, 759.
16. Y. Hoshino, H. Koide, K. Furuya, W. W. Haberaecker 3rd, S. H. Lee, T. Kodama, H. Kanazawa, N. Oku and K. J. Shea, *Proc. Natl. Acad. Sci. U.S.A.*, 2012, 109, 33.
17. J. A. H. Junghanns and R. H. Müller, *Int. J. Nanomedicine*, 2008, 3, 295.
18. B. E. Rabinow, *Nat. Rev. Drug Discov.*, 2004, 3, 785.
19. W. T. Lim, E. H. Tan, C. K. Toh, S. W. Hee, S. S. Leong, P. C. S. Ang, N. S. Wong and B. Chowbay, *Ann. Oncol.*, 2010, 21, 382.
20. E. Miele, G. P. Spinelli, E. Miele, F. Tomao, S. Tomao, *Int. J. Nanomedicine*, 2009, 4, 99.
21. A. Gabizon, H. Shmeeda, Y. Barenholz, *Clin. Pharmacokinet.*, 2003, 42, 419.

22. J. Hrkach, D. Von Hoff, M. Mukkaram Ali, E. Andrianova, J. Auer, T. Campbell, D. De Witt, M. Figa, M. Figueiredo, A. Horhota, S. Low, K. McDonnell, E. Peeke, B. Retnarajan, A. Sabnis, E. Schnipper, J. J. Song, Y. H. Song, J. Summa, D. Tompsett, G. Troiano, T. Van Geen Hoven, J. Wright, P. LoRusso, P. W. Kantoff, N. H. Bander, C. Sweeney, O. C. Farokhzad, R. Langer and S. Zale, *Sci. Transl. Med.*, 2012, 4, 128ra39.
23. C. Mamot, R. Ritschard, A. Wicki, G. Stehle, T. Dieterle, L. Bubendorf, C. Hilker, S. Deuster, R. Herrmann and C. Rochlitz, *Lancet Oncol.*, 2012 , 13, 1234.
24. P. J. Gaillard, B. M. Kerklaan, P. Aftimos, S. Altintas, A. Jager, W. Gladdines, F. Lonnqvist, P. Soetekouw, H. Verheul, A. Awada, J. Schellens and D. Brandsma, *Cancer Res.*, 2014, 74, CT216.
25. M. K. Yu, J. Park and S. Jon, *Theranostics*, 2012, 2, 3.
26. T. Coelho, D. Adams, A. Silva, P. Lozeron, P. N. Hawkins, T. Mant, J. Perez, J. Chiesa, S. Warrington, E. Tranter, M. Munisamy, R. Falzone, J. Harrop, J. Cehelsky, B. R. Bettencourt, M. Geissler, J. S. Butler, A. Sehgal, R. E. Meyers, Q. Chen, T. Borland, R. M. Hutabarat, V. A. Clausen, R. Alvarez, K. Fitzgerald, C. Gamba-Vitalo, S. V. Nochur, A. K. Vaishnaw, D. W. Sah, J. A. Gollob and O. B. Suhr, *New Engl. J. Med.*, 2013, 369, 819.
27. M. E. Davis, J. E. Zuckerman, C. H. Choi, D. Seligson, A. Tolcher, C. A. Alabi, Y. Yen, J. D. Heidel and A. Ribas, Nature, 2010, 464, 1067.
28. C. Butts, A. Maksymiuk, G. Goss, D. Soulières, E. Marshall, Y. Cormier, P. M. Ellis, A. Price, R. Sawhney, F. Beier, M. Falk and N. Murray, *J. Cancer Res. Clin. Oncol.*, 2011, 137, 1337.
29. P. O. Ilyinskii, C. J. Roy, C. P. O'Neil, E. A. Browning, L. A. Pittet, D. H. Altreuter, F. Alexis, E. Tonti, J. Shi, P. A. Basto, M. Iannacone, A. F. Radovic-Moreno, R. S. Langer, O. C. Farokhzad, U. H. von Andrian, L. P. Johnston and T. K. Kishimoto, *Vaccine*, 2014, 32, 2882.
30. K. K. Jain, *Drug Discov. Today*, 2005, 10, 1435.
31. E. C. Cho, C. Glaus, J. Chen, M. J. Welch and Y. Xia, *Trends Mol. Med.*, 2010, 16, 561.
32. M. A. Hahn, A. K. Singh, P. Sharma, S. C. Brown and B. M. Moudgil, *Anal. Bioanal. Chem.*, 2011, 399, 3.

33. J. Liu, M. Yu, C. Zhou and J. Zheng, *Mater. Today*, 2013; 16, 477.
34. J. Liu, M. Yu, X. Ning, C. Zhou, S. Yang and J. Zheng, *Angew. Chem. Int. Ed.*, 2013, 52, 12572.
35. J. Liu, M. Yu, C. Zhou, S. Yang, X. Ning and J. Zheng, *J. Am. Chem. Soc.*, 2013, 135, 4978.
36. S. Mura and P. Couvreur, *Adv. Drug Del. Rev.*, 2012, 64, 1394.
37. T. H. Kim, S. Lee, X. Chen, *Expert Rev. Mol. Diagn.*, 2013, 13, 257.
38. M. Lundqvist, J. Stigler, G. Elia, I. Lynch, T. Cedervall, K. A. Dawson, *Proc. Natl. Acad. Sci. U.S.A.*, 2008, 105, 14265.
39. S. Milani, F. B. Bombelli, A. S. Pitek, K. A. Dawson, and J. Rädler, *ACS Nano*, 2012, 6, 2532.
40. A. E. Nel, L. Mädler, D. Velegol, T. Xia, E. M. V. Hoek, P. Somasundaran, F. Klaessig, V. Castranova and M. Thompson, *Nat. Mater.*, 2009, 8, 543.
41. S. R. Saptarshi, A. Duschl and A. L. Lopata, *J. Nanobiotechnol.*, 2013, 11, 26.
42. N. Wangoo, C. R. Suri and G. Shekhawat, *Appl. Phys. Lett.*, 2008, 92, 133104.
43. Z. N. Gheshlaghi, G. H. Riazi, S. Ahmadian, M. Ghafari, R. Mahinpou, *Acta Biochim. Biophys. Sin.*, 2008, 40, 777.
44. M. Mahmoudi, M. A. Shokrgozar, S. Sardari, M. K. Moghadam, H. Vali, S. Laurent and P. Stroeve, *Nanoscale*, 2011, 3, 1127.
45. L. Treuel, S. Brandholt, P. Maffre, S. Wiegele, L. Shang and G. U. Nienhaus, *ACS Nano*, 2014, 8, 503.
46. A. Gessner, A. Lieske, B. Paulke, R. Müller, *Eur. J. Pharm. Biopharm.*, 2002, 54, 165.
47. C. D. Walkey, J. B. Olsen, H. Guo, A. Emili and W. C. Chan, *J. Am. Chem. Soc.*, 2012, 134, 2139.
48. C. Fang, B. Shi, Y. Y. Pei, M. H. Hong, J. Wu, H. Z. Chen, *Eur. J. Pharm. Sci.*, 2006, 27, 27.
49. P. Varallyay, G. Nesbit, L. L. Muldoon, R. R. Nixon, J. Delashaw, J. I. Cohen, A. Petrillo, D. Rink and E. A. Neuwelt, *Am. J. Neuroradiol.*, 2002, 23, 510.
50. C. Chouly, D. Pouliquen, I. Lucet, J. J. Jeune and P. J. Jallet, *J. Microencapsul.*, 1996, 13, 245.
51. Z. J. Deng, M. Liang, I .Toth, M. Monteiro and R. F. Minchin, *Nanotoxicology*, 2013, 7, 314.

52. A. Gessner, A. Lieske, B. Paulke and R. Muller, *J. Biomed. Mater. Res. A.*, 2003, 65A, 319.
53. A. A. Vertegel, R. W. Siegel and J. S. Dordick, *Langmuir*, 2004, 20, 6800.
54. Z. Deng, G. Mortimer, T. Schiller, A. Musumeci, D. Martin and R. Minchin, *Nanotechnology*, 2009, 20, 455101.
55. M. S. Ehrenberg, A. E. Friedman, J. N. Finkelstein, G. Oberdorster and J. L. McGrath, *Biomaterials*, 2009, 30, 603.
56. M. A. Dobrovolskaia, P. Aggarwal, J. B. Hall and S. E. McNeil, *Mol. Pharm.*, 2008, 5, 487.
57. D. E. Owens III and N. A. Peppas, *Int. J. Pharm.*, 2006, 307, 93.
58. T. Ishida, H. Harashima and H. Kiwada, *Curr. Drug Metabol.*, 2001, 2, 397.
59. J. Kreuter, *J. Nanosci. Nanotechnol.*, 2004, 4, 484.
60. K. Ogawara, K. Furumoto, S. Nagayama, K. Minato, K. Higaki, T. Kai and T. Kimura, *J. Controlled Release*, 2004, 100, 451.
61. A. Akinc, W. Querbes, S. De, J. Qin, M. Frank-Kamenetsky, K. N. Jayaprakash, M. Jayaraman, K. G. Rajeev, W. L. Cantley, J. R. Dorkin, J. S. Butler, L. Qin, T. Racie, A. Sprague, E. Fava, A. Zeigerer, M. J. Hope, M. Zerial, D. W. Sah, K. Fitzgerald, M. A. Tracy, M. Manoharan, V. Koteliansky, A. de Fougerolles and M. A. Maier, *Mol. Ther.*, 2010, 18, 1357.
62. J. R. Dunkelberger and W. C. Song, *Cell Res.*, 2010, 20, 34.
63. J. Szebeni, *Toxicology*, 2005, 216, 106.
64. S. M. Moghimi and Z. S. Farhangrazi, *Nanomedicine: Nanotechnol. Biol. Med.*, 2013, 9, 458.
65. I. Bertholon, C. Vauthier and D. Labarre, *Pharm. Res.*, 2006, 23, 1313.
66. J. Szebeni, P. Bedocs, Z. Rozsnyay, Z. Weiszhár, R. Urbanics, L. Rosivall, R. Cohen, O. Garbuzenko, G. Báthori, M. Tóth, R. Bünger and Y. Barenholz, *Nanomedicine*, 2012, 8, 176.
67. C. Salvador-Morales, L. Zhang, R. Langer and O. C. Farokhzad, *Biomaterials*, 2009, 30, 2231.

68. M. M. Markiewski, B. Nilsson, K. N. Ekdahl, T. E. Mollnes, J. D. Lambris, *TRENDS Immunol.*, 2007, 28, 184.
69. M. M. Markiewski, R. A. DeAngelis and J. D. Lambris, *Mol. Immunol.*, 2006, 43, 45.
70. D. Mastellos, C. Andronis, A. Persidis and J. D. Lambris, Clin. Immunol. 2005, 115, 225.
71. P. Tan, F. W. Luscinskas and S. Homer-Vanniasinkam, *Eur. J. Vasc. Endovasc. Surg.*, 1999, 17, 373.
72. M. A. Dobrovolskaia and S. E. McNeil, *Nat. Nanotechnol.*, 2007; 2, 469.
73. M. M. Moghimi, A. C. Hunter and J. C. Murray, Pharmacol. Rev., 2001, 53, 283.
74. L. H. Reddy and P. Couvreur, *J Hepatol.*, 2011, 55, 1461.
75. S. W. Jones, R. A. Roberts, G. R. Robbins, J. L. Perry, M. P. Kai, K. Chen, T. Bo, M. E. Napier, J. P. Y. Ting, J. M. DeSimone and J. E. Bear, *J. Clin. Invest.*, 2013, 123, 3061.
76. C. D. Mills, K. Kincaid, J. M. Alt, M. J. Heilman, A. M. Hill, *J. Immunol.*, 2000, 164, 6166.
77. D. V. Bazile, M. T. Bassoulet, M. Marlard, G. Splenlehauer and M. Veillard, *J. Pharm. Sci. Technol. Japan*, 1993, 53 suppl., 10.
78. R. Gref, Y. Minamitake, M. T. Peracchia, V. Trubetskoy, V. Torchilin and R. Langer, *Science*, 1994, 263, 1600.
79. S. I. Jeon, J. H. Lee, J. D. Andrade and P. G. De Gennes, *J. Colloid Interface Sci.*, 1991, 142, 149.
80. R. Gref, M. Luck, P. Quellec, M. Marchand, E. Dellacherie, S. Harnisch, T. Blunk and R. H Muller, *Coll. Surf. B: Biointerfaces*, 2000, 18, 301.
81. D. Bazile, C. Prud'homme, M. T. Bassoullet, M. Marlard, G. Spenlehauer and M. Veillard, *J. Pharm. Sci.*, 1995, 84, 493.
82. Laverman, P., et al. (2001). Factors affecting the accelerated blood clearance of polyethylene glycol-liposomes upon repeated injection. J. Pharmacol. Exp. Ther. 298: 607–612
83. R. Saadati, S. Dadashzadeh, Z. Abbasian and H. Soleimanjahi, *Pharm. Res.*, 2013, 30, 985.
84. T. L. Cheng, P. Y. Wu, M. F. Wu, J. W. Chern and S. R. Roffler, *Bioconj. Chem.*, 1999, 10, 520.

85. A. W. Richter and E. Akerblom, *Int. Arch. Allergy Appl. Immunol.*, 1984, 74, 36.
86. J. K. Armstrong, G. Hempel, S. Koling, L. S. Chan, T. Fisher, H. J. Meiselman and G. Garratty, *Cancer*, 2007, 110, 103.
87. H. Schellekens, W. E. Hennink and V. Brinks, *Pharm. Res.*, 2013, 30, 1729.
88. T. Ishida, X. Wang, T. Shimizu, K. Nawata and H. Kiwada, *J. Control. Release*, 2007, 122, 349.
89. X. Wang, T. Ishida and H. Kiwada, *J. Control. Release*, 2007, 119, 236.
90. Sherman MR, Williams LD, Sobczyk MA, Michaels SJ, Saifer MGP. Role of the Methoxy Group in Immune Responses to mPEG-Protein Conjugates. Bioconjug Chem. 2012, 23: 485-499.
91. T. Ishihara, M. Takeda, H. Sakamoto, A. Kimoto, C. Kobayashi, N. Takasaki, K. Yuki, K. Tanaka, M. Takenaga, R. Igarashi, T. Maed, N. Yamakawa, Y. Okamoto, M. Otsuka, T. Ishida, H. Kiwada, Y. Mizushima and T. Mizushima, *Pharm. Res.*, 2009, 26, 2270.
92. F. Gentile, M. Ferrari and P. Decuzzi, *Ann. Biomed. Eng.*, 2008, 36, 254.
93. T. Horn, J. H. Henriksen and P. Christoffersen, *Liver Int.*, 1986, 6, 98.
94. E. Igarashi, Factors affecting toxicity and efficacy of polymeric nanomedicines. *Toxicol. Appl. Pharmacol.*, 2008, 229, 121.
95. S. M. Moghimi and I. Hamad, Factors controlling pharmacokinetics of intravenously injected nanoparticulate Ssystems, in *Nanotechnology in drug delivery Biotechnology : Pharmaceutical aspects*, ed. M. M. de Villiers, P. Aramwit, and G. S. Kwon, Springer, New York, 2009, Volume X, 267-282.
96. H. Sarin, *J. Angiogenesis Res.*, 2010, 2, 14.
97. H. S. Choi, W. Liu, P. Misra, E. Tanaka, J. P. Zimmer, B. I. Ipe, M. G. Bawendi and J. V. Frangioni, *Nat. Biotechnol.*,2007, 25, 1165.
98. C. H. J. Choi, J. E. Zuckerman, P. Webster and M. E. Davis, *Proc. Natl. Acad. Sci. USA.*, 2011, 108, 6656.
99. T. Fujita, M. Nishikawa, Y. Ohtsubo, J. Ohno, Y. Takakura, H. Sezaki and M. Hashida, *J. Drug Targeting*, 1994, 2, 157.
100. S. D. Li and L. Huang, *Mol. Pharm.*, 2008, 5, 496.

101. T. S. Levchenko, R. Rammohan, A. N. Lukyanov, K. R. Whiteman and V.P. Torchilin, *Int. J. Pharm.*, 2002, 240, 95.

102. R. Kedmi, N. Ben-Arie and D. Peer, *Biomaterials*, 2010, 31, 6867.

103. J. A. Champion, S. Mitragotri, *Proc. Natl. Acad. Sci. U S A.*, 2006, 103, 4930.

104. J. A. Champion, S. Mitragotri, *Pharm. Res.*, 2009, 26, 244.

105. S. Tollis, A. E. Dart, G. Tzircotis and R. G. Endres, *BMC Syst. Biol.*, 2010, 4, 149.

106. Y. Geng, P. Dalhaimer, S. Cai, R. Tsai, M. Tewari, T. Minko and D. E. Discher, *Nat. Nanotechnol.*, 2007, 2, 249.

107. A. Maksimenko, F. Dosio, J. Mougin, A. Ferrero, S. Wack, L. H. Reddy, A. A. Weyn, E. Lepeltier, C. Bourgaux, B. Stella, L. Cattel and P. Couvreur, *Proc. Natl. Acad. Sci. U S A.*, 2014, 111, E217.

108. Z. Chu, S. Zhang, B. Zhang, C. Zhang, C. Y. Fang, I. Rehor , P. Cigler, H. C. Chang, G. Lin, R. Liu and Q. Li, *Sci. Rep.*, 2014, 4, Article number 4495.

109. R. E. Yanes, D. Tarn, A. A. Hwang, D. P. Ferris, S. P. Sherman, C. R. Thomas, J. Lu, A. D. Pyle, J. I. Zink and F. Tamanoi, *Small*, 2013, 9, 697.

110. K. C. L. Black, Y. Wang, H. P. Luehmann, X. Cai, W. Xing, B. Pang, Y. Zhao, C. S. Cutler, L. V. Wang, Y. Liu and Y. Xia, *ACS Nano*, 2014, 8, 4385.

111. K. A. Beningo and Y. L. Wang, Fc-receptor-mediated phagocytosis is regulated by mechanical properties of the target. *J. Cell Sci.*, 2002, 115, 849.

112. K. Shimizu, Y. Maitani, K. Takayama and T. Nagai, *J. Drug Target.*, 1996, 4, 245.

113. Igarashi, in Nanomedicines and nanoproducts – Applications, disposition and toxicology in human body, ed. E. Igarashi, CRC press, Boca Raton, Florida, 2015, pp. 165-216.

114. K. Muramatsu, Y. Maitani, K. Takayama and T. Nagai, *Drug Dev. Ind. Pharm.*, 1999, 25, 1099.

115. K. Muramatsu, T. Masumizu, Y. Maitani, S. H. Hwang, M. Kohno, K. Takayama and T. Nagai, *Chem. Pharm. Bull. (Tokyo),* 2000, 48, 610.

116. S. M. Moghimi and H. M. Patel, *FEBS Lett.*, 1988, 233, 143.

117. S. C. Semple, S. K. Klimuk, T. O. Harasym, N. Dos Santos, S. M. Ansell, K. F. Wong, N. Maurer, H. Stark, P. R. Cullis, M. J. Hope, P. Scherrer, *Biochim. Biophys. Acta*, 2001, 1510, 152.

118. D. E. Discher and F. Ahmed, *Annu. Rev. Biomed. Eng.*, 2006, 8, 323.

119. H. M. Burt, X. Zhang, P. Toleikis, L. Embree and W. L. Hunter, *Coll. Surf. B: Biointerfaces*, 1999, 16, 161.

120. S. K. Sahoo, J. Panyam, S. Prabha, V. Labhasetwar, *J. Control. Release*, 2002, 82, 105.

121. L. Horev-Azaria, C. J. Kirkpatrick, R. Korenstein, P. N. Marche, O. Maimon, J. Ponti, R. Romano, F. Rossi, U. Golla-Schindler, D. Sommer, C. Uboldi, R. E. Unger and C. Villiers, *Toxicol. Sci.*, 2011, 122, 489.

122. T. Mosmann, *J. Immunol. Methods*, 1983, 65, 55.

123. J. C. Stockert, A. Blazquez-Castro, M. Canete, R. W. Horobin and A. Villanueva, *Acta Histochemica*, 2012, 114, 785.

124. N. J. Marshall, C. J. Goodwin, S. J. Holt, *Growth Regul.*, 1995, 5, 69.

125. M. Natarajan, S. Mohan, B. R. Martinez, M. L. Meltz and T. S. Herman, *Cancer Detect. Prev.*, 2000, 24, 405.

126. P. Takhar and S. Mahant, *Arch. Appl. Sci. Res.*, 2011, 3, 389.

127. J. O'Brien, I. Wilson, T. Orton and F. Pognan, *Eur. J. Biochem.*, 2000, 267, 5421.

128. L. Horev-Azaria, G. Baldi, D. Beno, D. Bonacchi, U. Golla-Schindler, J. C. Kirkpatrick, S. Kolle, R. Landsiedel, O. Maimon, P. N. Marche, J. Ponti, R. Romano, F. Rossi, D. Sommer, C. Uboldi, R. E. Unger, C. Villiers and R. Korenstein, *Particle and Fibre Toxicol.*, 2013, 10, 32.

129. U.S. Pat., 5 501 959, 1996.

130. S. M. Hussain and J. M. Frazier, *Toxicol. Sci.*, 2002, 69, 424.

131. V. W. Hu, G. E. Black, A. Torres-Duarte and F. P. Abramson, *FASEB J.*, 2002, 16, 1456.

132. J. M. Hillegass, A. Shukla, S. A. Lathrop, M. B. MacPherson, N. K. Fukagawa and B. T. Mossman, *Wiley Interdiscip. Rev. Nanomed. Nanobiotechnol.*, 2010, 2, 219.

133. E. Herzog, A. Casey, F. M. Lyng, G. Chambers, H. J. Byrne and M. Davoren, *Toxicol. Lett.*, 2007, 174, 49.

134. M. Huang, E. Khor and L. Y. Lim, *Pharmacol. Res.*, 2004, 21, 344.

135. K. Kostarelos, L. Lacerda, G. Pastorin, W. Wu, S. Wieckowski, J. Luangsivilay, S. Godefroy, D. Pantarotto, J. P. Briand, S. Muller, M. Prato and A. Bianco, *Nat. Nanotechnol.*, 2007, 2, 108.

136. W. F. Vevers and A. N. Jha, *Ecotoxicology*, 2008, 17, 410.

137. V. Sharma, D. Anderson and A. Dhawan, *Apoptosis*, 2012, 17, 852.

138. W. Strober, *Curr. Protocols Immunol.*, 2001, Appendix 3: Appendix 3B.

139. V. Katsares, A. Petsa, A. Felesakis, Z. Paparidis, E. Nikolaidou, S. Gargani, I. Karvounidou, K. A. Ardelean, N. Grigoriadis, J. Grigoriadis, *LabMedicine*, 2009, 40, 557.

140. S. Kanagesan, M. Hashim, S. Tamilselvan, N. B. Alitheen, I. Ismail and G. Bahmanrokh, *J. Nanomaterials.*, 2013, 2013 Article ID 865024, 8 pages.

141. L. H. Reddy, J. M. Renoir, V. Marsaud, S. Lepetre-Mouelhi, D. Desmaële, P. Couvreur, *Mol. Pharm.*, 2009, 6, 1526.

142. G. Repetto, A. del Peso and J. L. Zurita, *Nat. Protocol.*, 2008, 3, 1125.

143. C. M. Sayes, J. D. Fortner, W. Guo, D. Lyon, A. M. Boyd, K. D. Ausman, Y. J. Tao, B. Sitharaman, L. J. Wilson, J. B. Hughes, J. L. West and V. L. Colvin, *Nano Lett.*, 2004, 4, 1881.

144. L. R. Hirsch, R. J. Stafford, J. A. Bankson, S. R. Sershen, B. Rivera, R. E. Price, J. D. Hazle, N. J. Halas and J. L. West, *Proc. Natl. Acad. Sci. U. S. A.*, 2003, 100, 13549.

145. Kaneshiro ES, Wyder MA, Wu YP, Cushion MT. Reliability of calcein acetoxy methyl ester and ethidium homodimer or propidium iodide for viability assessment of microbes. J. Microbiol. Methods, 1993, 17, 1-16.

146. Y. Luo, W. Chaoming, Y. Qiao, M. Hossain, L. Ma and M. Su, *J. Mater. Sci: Mater. Med.*, 2012, 23, 2563.

147. L. Braydich-Stolle, S. Hussain, J. J. Schlager and M.C. Hofmann, *Toxicol. Sci.*, 2005, 88, 412.

148. Fadok VA, Bratton DL, Frasch SC, Warner ML, Henson PM. The role of phosphatidylserine in recognition of apoptotic cells by phagocytes. *Cell Death Diff.*, 1998; 5: 551-562.

149. X. Lu, J. Qian, H. Zhou, Q. Gan, W. Tang, J. Lu, Y. Yuan and C. Liu, *Int. J. Nanomedicine*, 2011, 6, 1889.

150. L. H. Reddy, J. S. Adhikari, B. S. R. Dwarakanath, R. K. Sharma and R. R. Murthy, *The AAPS J.*, 2006, 8 (2) Article 29.

151. C. D. Bortner, N. B. Oldenburg and J. A. Cidlowski, *Trends Cell Biol.*, 1995, 5, 21.

152. B. B. Wolf, M. Schuler, F. Echeverri and D. R. Green, *J. Biol. Chem.*, 1999, 274, 30651.

153. S. Arora, J. Jain, J. M. Rajwade and K. M. Paknikar, *Toxicol. Lett.*, 2008, 179, 93.

154. Y. A. Loannou and F. W. Chen, *Nucl. Acids Res.*, 1996, 24, 992.

155. S. Chandna, *Cytometry A*, 2004, 61, 127.

156. Z. Darzynkiewicz, D. Galkowski and H. Zhao, *Methods*, 2008, 44, 250.

157. T. Sun, Y. Yan, Y. Zhao, F. Guo and C. Jiang, *PLoS ONE*, 2012, 7, e43442.

158. W. Kai, X. Xiaojun, P. Ximing, H. Zhenqing, and Z. Qiqing, *Nanoscale Res. Lett.*, 2011, 6, 480.

159. S. Kamada, H. Kusano, H. Fujita, M. Ohtsu, R. C. Koya, N. Kuzumaki and Y. Tsujimoto, *Proc. Natl. Acad. Sci. USA*, 1998, 95, 8532.

160. A. G. Porter and R. U. Janicke, *Cell Death Differ.*, 1999, 6, 99.

161. L. Foucaud, M. R. Wilson, D. M. Brown and V. Stone, *Toxicol. Lett.*, 2007, 174, 1.

162. C. C. Huang, R. S. Aronstam, D. R. Chen, Y. W. Huang, *Toxicol. in Vitro*, 2010, 24, 45.

163. M. J. Akhtar, S. Kumar, R. C. Murthy, M. Ashquin, M. I. Khan, G. Patil, I. Ahmad, *Toxicol. in Vitro*, 2010, 24, 1139.

164. B. C. Heng, X. Zhao, E. C. Tan, N. Khamis, A. Assodani, S. Xiong, C. Ruedl, K. W. Ng and J. S. Loo, *Arch. Toxicol.*, 2011, 85, 1517.

165. R. P. Schins, R. Duffin, D. Höhr, A. M. Knaapen, T. Shi, C. Weishaupt, V. Stone, K. Donaldson and P. J. Borm, *Chem. Res. Toxicol.*, 2002, 15, 1166.

166. I. Papageorgiou, C. Brown, R. Schins, S. Singh, R. Newson, S. Davis, J. Fisher, E. Ingham and C. P. Case, *Biomaterials*, 2007, 28, 2946.

167. S. Singh, T. Shi, R. Duffin, C. Albrecht, D. van Berlo, D. Höhr, B. Fubini, G. Martra, I. Fenoglio and P. J. Borm, R. P. Schins, *Toxicol. Appl. Pharmacol.*, 2007, 222, 141.

168. K. Bhattacharya, M. Davoren, J. Boertz, R. P. F. Schins, E. Hoffman and E. Dopp, *Particle and Fibre Toxicol.*, 2009, 6, 17.

169. P. S. Gilmour, P. H. Beswick, D. M. Brown and K. Donaldson, *Carcinogenesis*, 1995, 16, 2973.

170. P. S. Gilmour, D. M. Brown, P. H. Beswick, W. MacNee, I. Rahman and K. Donaldson, *Environ. Health Perspect.*, 1997, 105(Suppl 5), 1313.

171. V. Stone, H. Johnston and M. J. Clift, *IEEE Trans. Nanobioscience*, 2007, 6, 331.

172. V. Stone, H. Johnston, R. P. Schins, *Crit. Rev. Toxicol.*, 2009, 39, 613.

173. S. Aula, S. Lakkireddy, A. V. N. Swamy, A. Kapley, K. Jamil, N. R. Tata and K. Hembram, *Mater. Res. Exp.*, 2014, 1, 035041.

174. S. H. Lee, J. E. Pie, Y. R. Kim, H. R. Lee, S. W. Son and M. K. Kim, Mol. Cell Toxicol., 2012, 8, 113.

175. S, Alarifi, D. Ali, S. Alkahtani, A. Verma, M. Ahamed, M. Ahmed and H. A. Alhadlaq, *Int. J. Nanomedicine*, 2013, 8, 983.

176. Y. Sun, L.W. Oberley and Y. Li, *Clin. Chem.*, 1988, 34, 497.

177. P. Chelikani, I. Fita and P. C. Loewen, *Cell. Mol. Life Sci.*, 2004, 61, 192.

178. B. Fahmy and S. A. Cormier, *Toxicol. In Vitro*, 2009, 23, 1365.

179. J. Lakritz, C. G. Plopper and A. R. Buckpitt, *Anal. Biochem.*, 1997, 247, 63.

180. C. M. Sayes, A. M. Gobin, K. D. Ausman, J. Mendez, J. L. West and V. L. Colvin, *Biomaterials*, 2005, 26, 7587.

181. J. R. Arthur, *Cell. Mol. Life Sci.*, 2000, 57, 1825.

182. R. Meena, R. Pal, S. N. Pradhan, M. Rani and R. Paulraj, *Adv. Mat. Lett.*, 2012b, 3, 459.

183. M. Radu, M. C. Munteanu, S. Petrache, A. I. Serban, D. Dinu, A. Hermenean, C. Sima and A. Dinischiotu, *Acta Biochim. Polonica*, 2010, 57, 355.

184. B. Wu and D. Dong, *Trends Pharmacol. Sci.*, 2012, 33, 656.

185. W. H. Habig, M. J. Pabst and W. B. Jakoby, *J. Biol. Chem.*, 1974, 249, 7130.

186. D. R. Janero, *Free Radical Biol. Med.*, 1990, 9, 515.

187. P.V. Asharani, M. P. Hande and S. Valiyaveettil, *BMC Cell Biol.*, 2009, 10, 65.

188. H. Nabeshi, T. Yoshikawa, K. Matsuyama, Y. Nakazato, S. Tochigi, S. Kondoh, T. Hirai, T. Akase, K. Nagano, Y. Abe, Y. Yoshioka, H. Kamada, N. Itoh, S. Tsunoda and Y. Tsutsumi *Particle Fibre Toxicol.*, 2011, 8, 1.

189. B. N. Ames, W. E. Durston, E. Yamasaki and F. D. Lee, *Proc. Natl. Acad. Sci. USA*, 1973, 70, 2281.

190. H. R. Kim, Y. J. Park, D. Y. Shin, S. M. Oh and K. H. Chung, Environ. Health. Toxicol., 2013, 28, e2013003.

191. R. Landsiedel, M. D. Kapp, M. Schulz, K. Wiench and F. Oesch, *Mutat. Res.*, 2009, 681, 241.

192. K. Chu, M. J. Tsai, *Diabetes*, 2005, 54, 1064.

193. X. Kong, G. R. Hellermann, W. Zhang, P. Jena, M. Kumar, A. Behera, S. Behera, R. Lockey, S. S. Mohapatra, *Allergy Asthma Clin. Immunol.*, 2008, 4, 95.

194. M. J. Holden and L. Wang, Quantitative Real Time PCR: Fluorescent Probe Options and Issues. In: Standardization and Quality Assurance in Fluorescence Measurements: Bioanalytical and Biomedical Applications, in *Fluorescence: Methods and Applications*, ed. U. Resch-Genger, Springer-Verlag, Berlin, 2008, 6, 489-508.

195. M. J. Akhtar, M. Ahamed, S. Kumar, M. A. M. Khan, J. Ahmad, S. A. Alrokayan, *Int. J. Nanomedicine*, 2012, 7, 845.

196. Y. Zhang, Z. Hu, M. Ye, Y. Pan, J. Chen, Y. Luo, Y. Zhang, L. He and J. Wang, *Eur. J. Pharm. Biopharm.*, 2007, 66, 268.

197. M. A. Dobrovolskaia, J. D. Clogston, B. W. Neun, J. B. Hall, A. K. Patri and S. E. McNeil, *Nano Lett.*, 2008, 8, 2180.

198. S. M. Moghimi, *J. Control. Release*, 2014, 190, 556.

199. M. Vittaz, D. Bazile, G. Spenlehauer, T. Verrecchia, M. Veillard, F. Puisieux and D. Labarre, Biomaterials, 1996, 17, 1575.

200. J. Szebeni, L. Baranyi, S. Savay, J. Milosevits, M. Bodo, R. Bunger, C. R. Alving, *Methods Enzymol.*, 2003, 373, 136.

201. J. Szebeni, P. Bedőcs, D. Csukás, L. Rosivall, R. Bünger, R. Urbanics, *Adv. Drug Deliv. Rev.*, 2012, 64, 1706.

202. I. Hamad, A. C. Hunter and S. M. Moghimi, *J. Control. Release*, 2013, 170, 167.

203. A. N. Ilinskaya and M. A. Dobrovolskaia, *Nanomedicine (Lond)*, 2013, 8, 969.

204. H. Sahli, J. Tapon-Bretaudière, A. M. Fischer, C. Sternberg, G. Spenlehauer, T. Verrecchia and D. Labarre, *Biomaterials*, 1997, 18, 281.

205. B. W. Neun, M. A. Dobrovolskaia, *Methods Mol. Biol.*, 2011, 697, 225.

206. T. T. W. Shwe, S. Yamamoto, M. Kakeyama, T. Kobayashi and H. Fujimaki, *Toxicol. Appl. Pharmacol.*, 2005, 209, 51.

207. C. M. Sayes, K. L. Reed, D. B. Warheit, *Toxicol. Sci.*, 2007, 97, 163.

208. P. Mantecca, G. Sancini, E. Moschini, F. Farina, M. Gualtieri, A. Rohr, G. Miserocchi, P. Palestini and M. Camatini, *Toxicol .Lett.*, 2009, 189, 206.

209. J. Leszczynski, *Nat. Nanotechnol.*, 2010, 5, 633.

210. P. P. Adiseshaiah, J. B. Hall and S. E. McNeil, *Wiley Interdiscip. Rev. Nanomed. Nanobiotechnol.*, 2010, 2, 99.

211. A. Monopoli, A. S. Pitek, I. Lynch and K. A. Dawson, Formation and Characterization of the Nanoparticle–Protein Corona, in *Nanomaterial Interfaces in Biology : Methods and Protocols*, Ed. P. Bergese and K. Hamad-Schifferli, Springer Humana press, New York, 2013, 1025, 137-155.

212. H. R. Kim, K. Andrieux, C. Delomenie, H. Chacun, M. Appel, D. Desmaële, F. Taran, D. Georgin, P. Couvreur and M. Taverna, *Electrophoresis*, 2007, 28, 2252.

213. D. Lorusso, A. Di Stefano, V. Carone, A. Fagotti, S. Pisconti, G. Scambia, *Ann. Oncol.*, 2007, 18, 1159.

214. N. Yokomichi, T. Nagasawa, A. Coler-Reilly, H. Suzuki, Y. Kubota, R. Yoshioka, A. Tozawa, N. Suzuki and Y. Yamaguchi, *Hum. Cell.*, 2013, 26, 8.

215. M. Longmire, P. L. Choyke and H. Kobayashi, *Nanomedicine (Lond).*, 2008, 3, 703.

216. T. Daemen, G. Hofstede, M. T. Ten Kate, I. A. J. M. Bakker-Woudenberg and G. L. Scherphof, *Int. J. Cancer*, 1995, 61, 761.

217. J. P. Plard and D. Bazile, *Coll. Surf. B: Biointerfaces*, 1999, 16, 173.

218. I. Hamad, A. Christy Hunter, K. J. Rutt, Z. Liu, H. Dai and S. Moein Moghimi, *Mol. Immunol.*, 2008, 45, 3797.

219. T. R. Downs, M. E. Crosby, T. Hu, S. Kumar, A. Sullivan, K. Sarlo, B. Reeder, M. Lynch, M. Wagner, T. Mills, S. Pfuhler, *Mutat. Res.*, 2012, 745, 38.

220. S. Ivanov, S. Zhuravsky, G. Yukina, V. Tomson, D. Korolev, M. Galagudza, *Materials*, 2012, 5, 1873.

221. M. A. K. Abdelhalim, B. M. Jarrar, *J. Nanobiotechnology*, 2012, 10, 5.

222. A. M. Prodan, S. L. Iconaru, C. S. Ciobanu, M. C. Chifiriuc , M. Stoicea and D. Predoi, *J. Nanomaterials*, 2013, 2013, Article ID 587021, 10 pages

223. K. M. A. Hassanin, S H. A. El-Kawi and K. S. Hashem, *Int. J. Nanomedicine*, 2013, 8, 1713.

224. J. S. Kim, J. H. Sung, J. H. Ji, K. S. Song, J. H. Lee, C. S. Kang and I. J. Yu, *Saf. Health Work*, 2011, 2, 34.

225. Z. Chen, Y. Wang, T. Ba, Y. Li, J. Pu, T. Chen, Y. Song, Y. Gu, Q. Qian, J. Yang and G. Jia, *Toxicol. Lett.*, 2014, 226, 314.

226. L. H. Reddy, P. E. Marque, C. Dubernet, S. L. Mouelhi, D. Desmaele and P. Couvreur. *Drug Metabol. Disp.*, 2008, 325, 484.

227. M. Li, K. T. Al-Jamal, K. Kostarelos and J. Reineke, *ACS Nano*, 2010, 4, 6303.

228. P. Espié, D. Tytgat, M. L. Sargentini-Maier, I. Poggesi and J. B. Watelet, *Drug Metab. Rev.*, 2009, 41, 391.

229. L. MacCalman, C. L. Tran and E. Kuempel, *J. Physics: Conference Series*, 2009, 151, 012028.

230. C. L. Tran, E. D. Kuempel and V. Castranova, *Ann. Occup. Hygiene*, 2002, 46(suppl 1), 14.

231. D. P. Lankveld, A. G. Oomen, P. Krystek, A. Neigh, A. Troost-de Jong, C. W. Noorlander, J. C. Van Eijkeren, R. E. Geertsma and W. H. De Jong, *Biomaterials*, 2010, 31, 8350.

232. H. A. Lee, T. L. Leavens, S. E. Mason, N. A. Monteiro-Riviere, J. E. Riviere, Nano Lett., 2009, 9, 794.

233. M. Li, Z. Panagi, K. Avgoustakis and J. Reineke, *Int. J. Nanomedicine*, 2012, 7, 1345.

234. P. Lin, J. W. Chen, L. W. Chang, J. P. Wu, L. Redding, H. Chang, T. K. Yeh, C. S. Yang, M. H. Tsai, H. J. Wang, Y. C. Kuo and R. S. Yang, *Environ. Sci. Technol.*, 2008, 42, 6264.

Tables

Table 1. Commercialized nanotechnology products for drug delivery and imaging.

Product	Technology	Route	Indication
Improve drug bioavailability/enable drug administration			
Rapamune	Nanocrystalline suspension of Rapamycin	Oral	Immunosuppressive
Tricor	Nanocrystalline suspension of Fenofibrate	Oral	Hypercholesterolemia
Triglide	Nanocrystalline suspension of Fenofibrate	Oral	Hypercholesterolemia
Emend	Nanocrystalline suspension of Aprepitant	Oral	Nausea and Emesis
Megace ES	Nanocrystalline suspension of Megestrol	Oral	Anorexia
Alter drug pharmacokinetics/achieve therapeutic benefit			
Marqibo	Sphingomyelin/cholesterol liposome (non-PEGylated) containing vincristine sulfate	Intravenous	Cancer
Abraxane	Albumin nanoparticle loaded with paclitaxel	Intravenous	Cancer
Invega Sustenna	Drug nanocrystalline suspension	Intramuscular	Schizophrenia
DepoCyt	Liposome containing cytarabine	Intravenous	Cancer
Ambisome	Liposome (non-PEGylated) containing Amphotericin B	Intravenous	Visceral leishmaniasis, fungal infections
Doxil / Caelyx	Liposome (PEGylated) containing doxorubicin HCl	Intravenous	Cancer
DaunoXome	Liposome (non-PEGylated) containing daunorubicin	Intravenous	Cancer
Myocet	Liposome (non-PEGylated) containing doxorubicin citrate	Intravenous	Cancer
Diprivan	Emulsion containing propofol	Intravenous	Anesthetic
Delivery of antigens / vaccines			
Fluad	Squalene-based oil-in-water nano-emulsion formulation containing Influenza / pandemic flu virus antigen	Intramuscular	Influenza
Pandemrix	AS03 adjuvant (oil-in-water emulsion made of α-tocopherol, squalene and polysorbate 80) loaded with H1N1 influenza antigen	Intramuscular	H1N1 influenza pandemic (flu)
Fendrix	AS04 adjuvant (dispersion of monophosphoryl lipid A and	Intramuscular	Hepatitis B viral infection

	aluminium phosphate) loaded with Hepatitis B surface antigen		
Epaxal	Reconstituted viral membrane vesicles containing the viral proteins and lipids loaded with inactivated Hepatitis A virus	Intramuscular	Hepatitis A virus infection
Inflexal® V	Reconstituted viral membrane vesicles containing the viral proteins and lipids loaded with influenza (subunit)	Intramuscular	Influenza
Cervarix	AS04 adjuvant (dispersion of monophosphoryl lipid A and aluminium phosphate) loaded with Human papilloma virus antigens (types 16 and 18)	Intramuscular	Cervical cancer caused by Human papilloma virus
Gardasil	Virus-like particles containing Human papilloma virus antigens (types 6, 11, 16, and 18)	Intramuscular	Cervical cancer caused by Human papilloma virus
Imaging			
Ferumoxsil /Lumirem	Iron oxide nanoparticle coated with dextran	Oral	Gastrointestinal imaging
Ferristene/Abdoscan	Iron oxide nanoparticle coated with sulfonated styrene−divinylbenzene copolymer	Oral	Gastrointestinal imaging
Ferumoxide/Endorem	Iron oxide nanoparticle coated with dextran	Intravenous	Liver imaging
Ferucarbotran/Resovist	Iron oxide nanoparticle coated with dextran	Intravenous	Liver imaging

Figures

Figure 1. Classification of nanoparticles for biomedical applicaitons

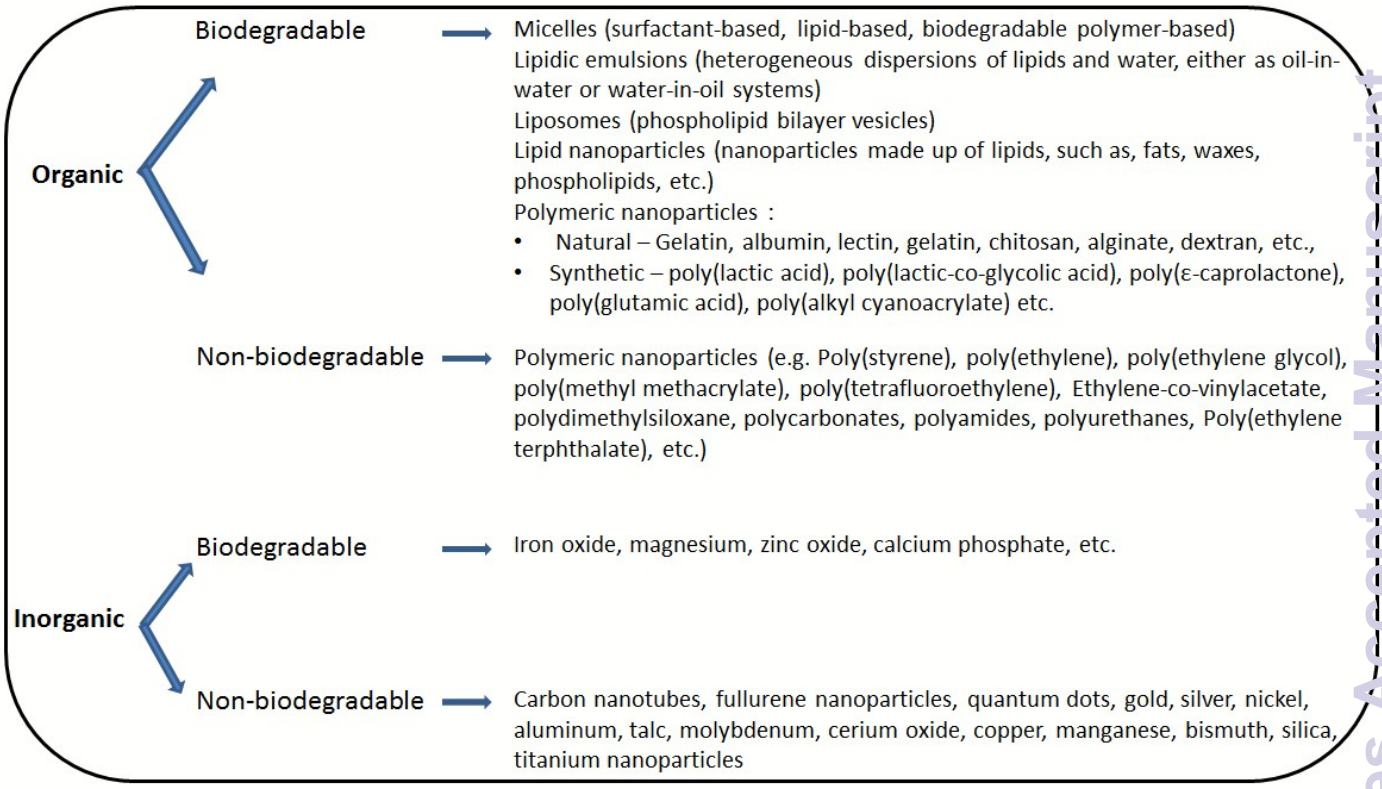

Figure 2. Schematic representation of the toxicity assessment of nanoparticles, *in vitro* and *in vivo*

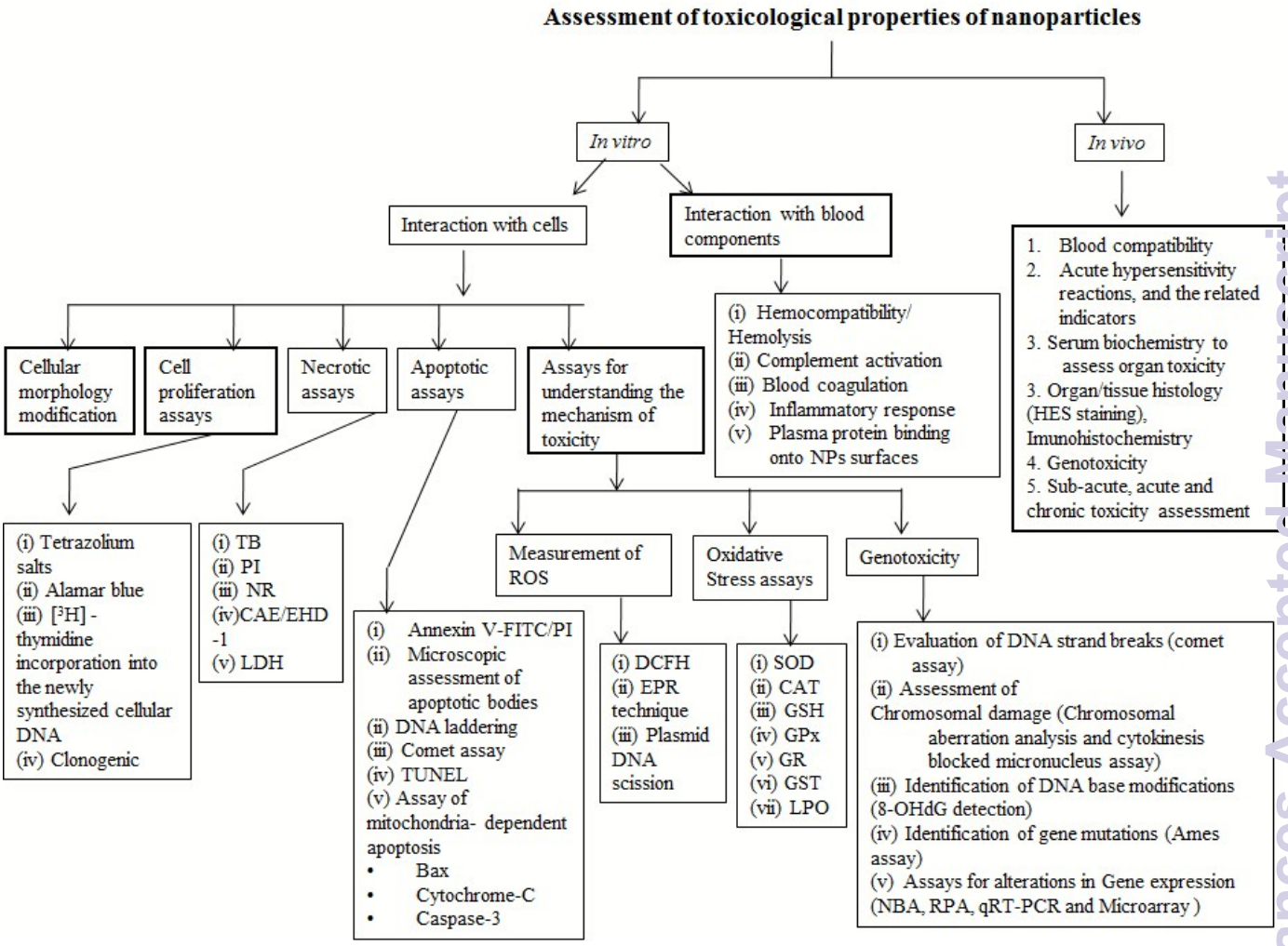

TB:Trypan blue; PI:Propidium iodide; NR:Neutral red; CAE-EHD-1: Calcein acetoxymethyl ester/ ethidium homodimer-1; LDH-Lactate dehydrogenase; Annexin V-FITC/PI: Annexin V-fluorescein isothiocyanate/ Propidium iodide; TUNEL- Terminal deoxynucleotidyl Transferase mediated dUTP-biotin Nick End Labeling; ROS: Reactive oxygen species; DCFH: 2,7-Dichlorodihydrofluorescein ;EPR: Electroparamagnetic resonance; SOD: Superoxide dismutase; CAT: Catalase; GSH-Glutathione; GPx: Glutathione peroxidase; GR: Glutathione reductase; GST:Glutathione-s-transferase;LPO:Lipid peroxidation;8-OHdG:8-hydroxyl-2'-deoxyguanosine; NPs: Nanoparticles; NBA: Northern blot analysis; RPA: Ribonuclease protection assay; qRT-PCR: Quantitative real-time polymerase chain reaction; HES: Hematoxylin Eosin and Saffran.

Figure 3. Intracellular reduction of MTT (3-(4, 5- dimethylthiazol-2- yl)-2, 5-diphenyltetrazolium bromide) to purple coloured formazan dye

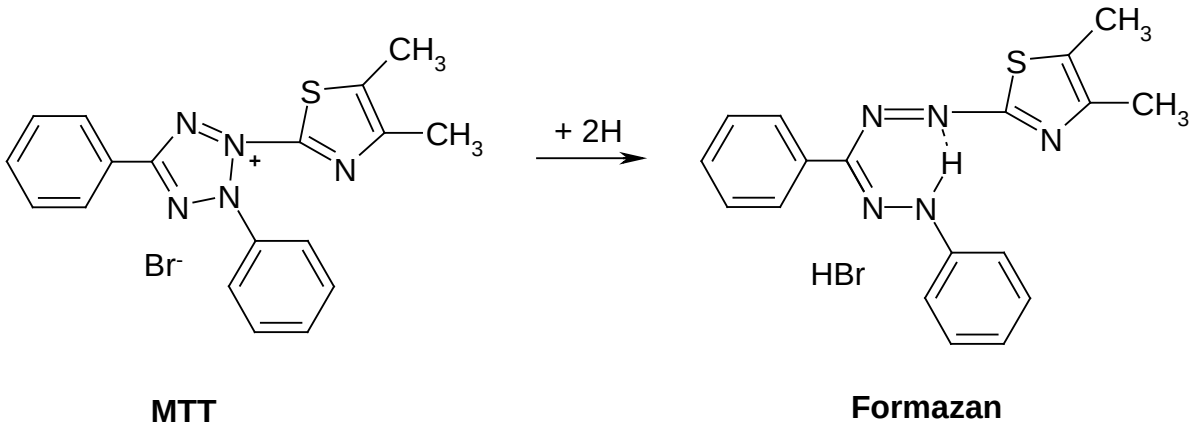

MTT **Formazan**

Figure 4. Reduction in viable cells, of non-fluorescent alamar blue (resazurin) to a bright red fluorescent resorufin.

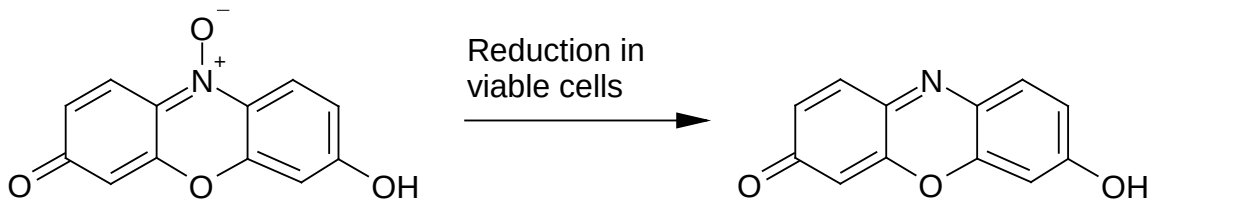

Resazurin (non-fluorescent compound) Resorufin (fluorescent compound)

Figure 5. Chemical structures of neutral red as neutral form and acidic form

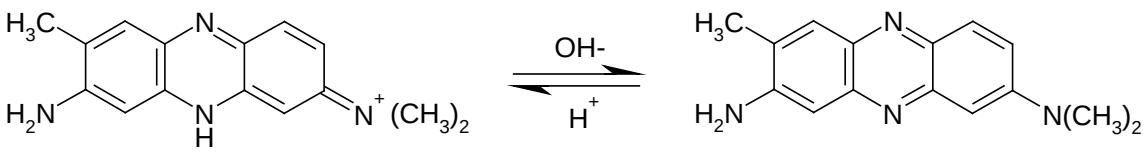

Neutral Red (acidic form) Neutral Red (neutral form)

Figure 6. Intracellular conversion of non-fluorescent calcein violet acetoxymethylester to the fluorescent anionic calcein violet by esterases in the living cells

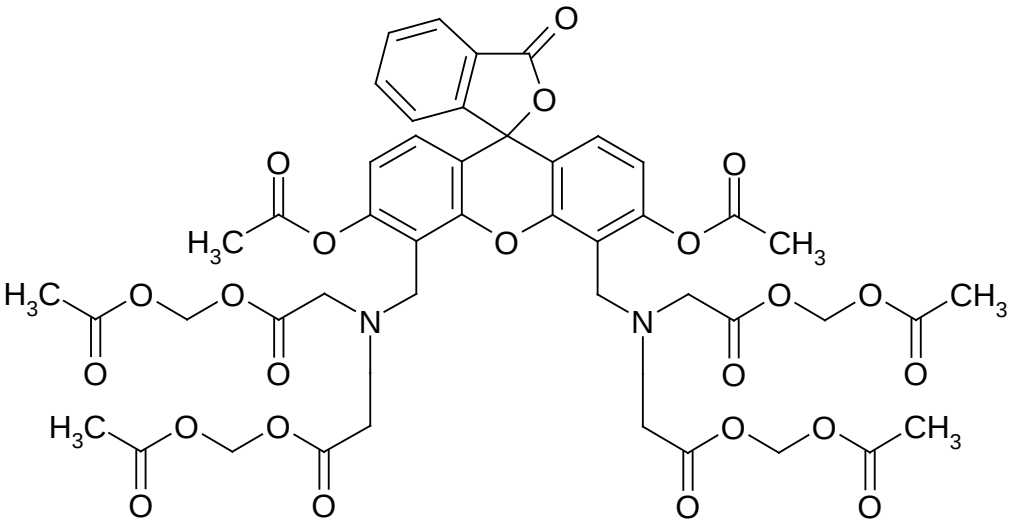

Calcein violet acetoxymethylester (non-fluorescent compound)

Intracellular esterases
(in the living cells)

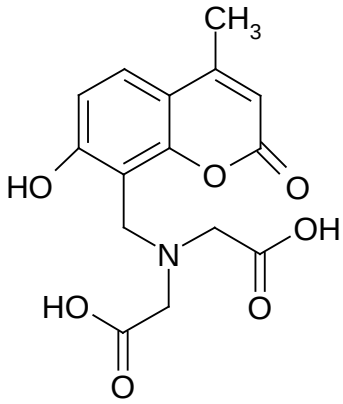

Calcein violet (fluorescent compound)

Figure 7. Ethidium homodimer (5,5'-[1,2-ethanediylbis(imino-3,1-propanediyl)]bis(3,8-diamino-6-phenyl) dichloride dihydrochloride) penetrate the dead cells and binds to DNA thereby exhibiting red fluorescence

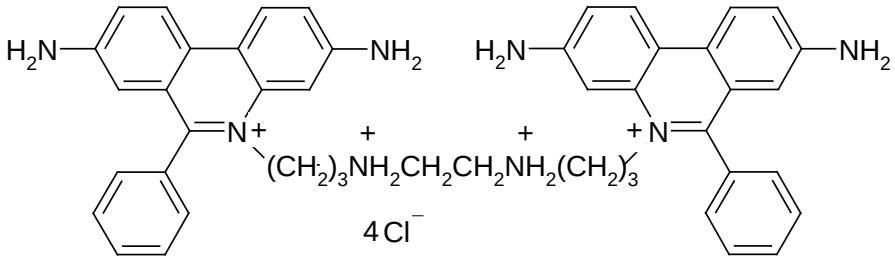

Ethidium homodimer (EthD-1)

Binds to DNA → Enhanced red fluorescence in the dead cells

Figure 8. Schematic representation of the formation of NADH in the living cells during lactate dehydrogenation (A), followed by the reaction between the so formed NADH and INT resulting in the formation of red colored INT formazan (B).

A

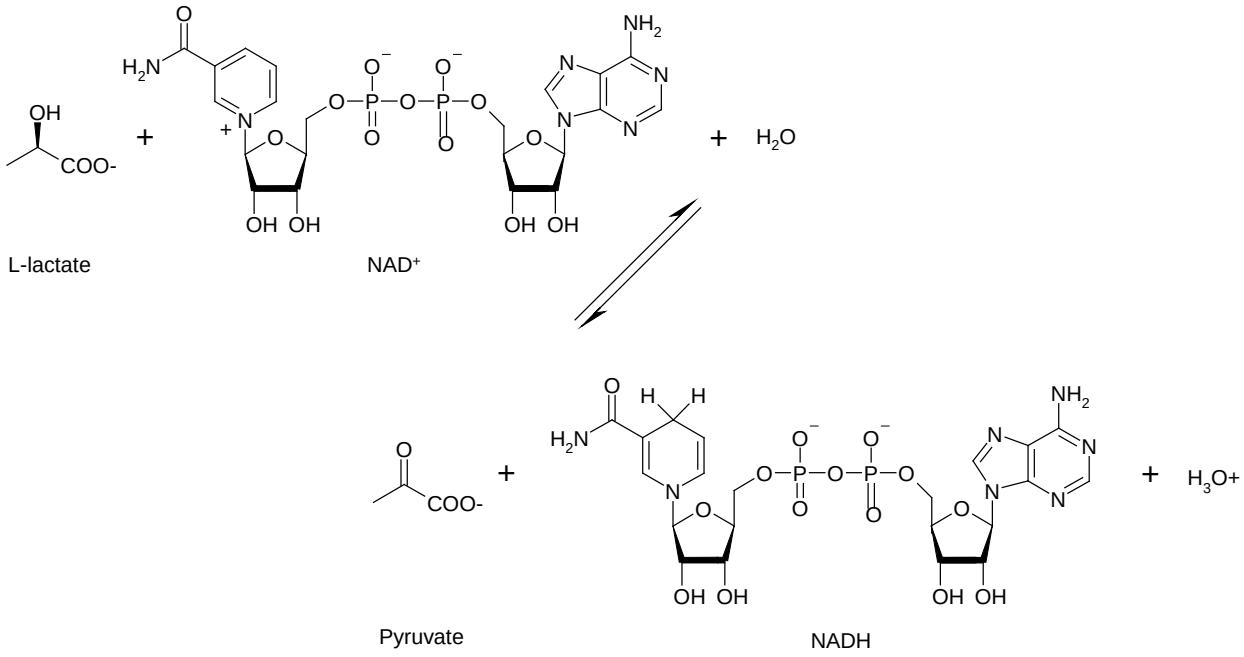

B

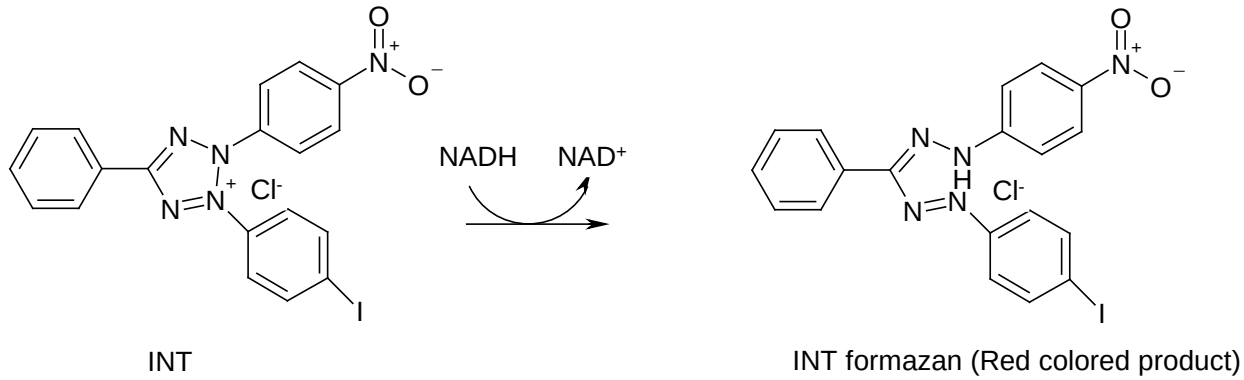

Figure 9. Illustration of apoptotic bodies in an apoptosis induced cell.

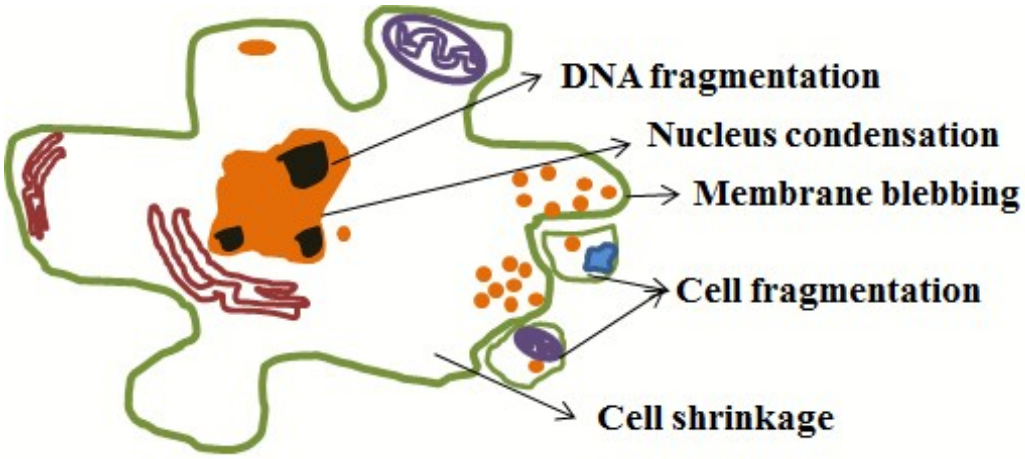

Figure 10. Structural representation of the conversion of the reagent DCFH-DA (2^1,7^1-dichlorofluorescein diacetate) to DCFH in the cells by esterases, and subsequent reaction of DCFH with intracellular reactive oxygen species resulting in the formation of fluorescent DCF (2^1,7^1-dichlorofluorescein).

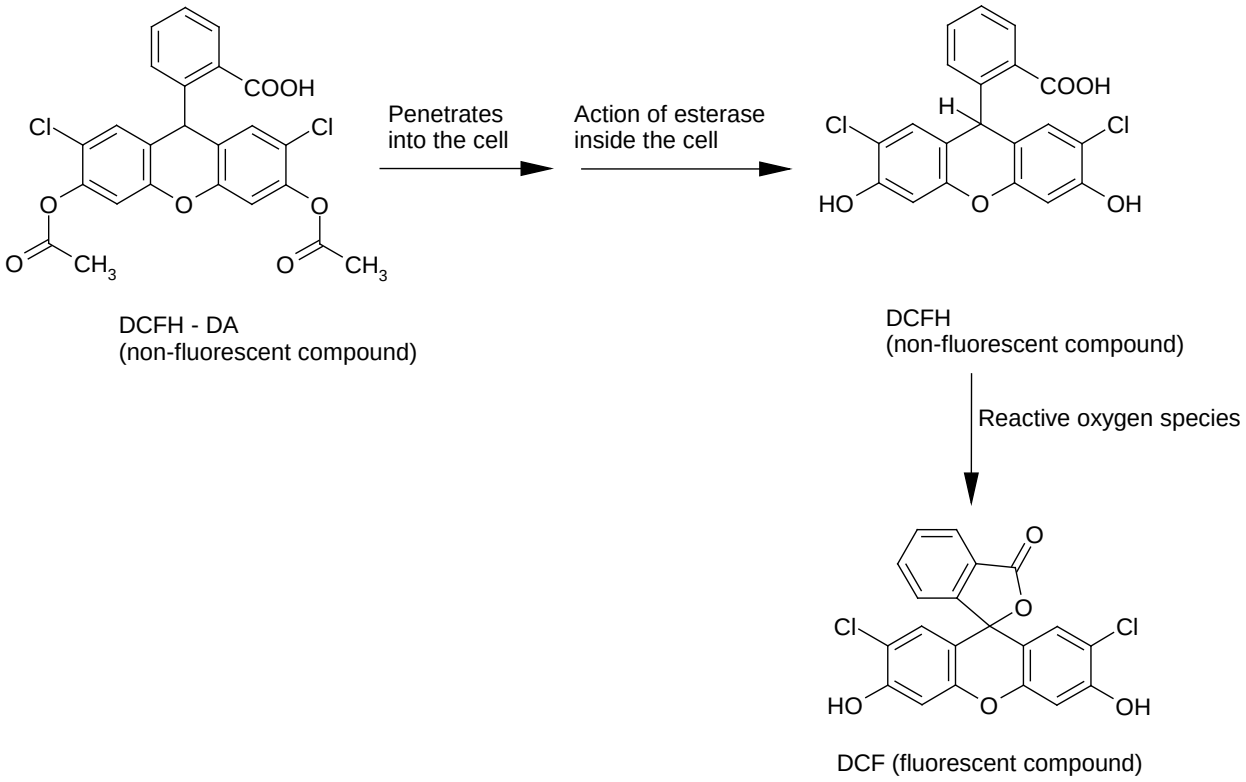

Figure 11. Schematic representation of the formation of formaldehyde from methanol by the action of catalase, and the interaction of so formed formaldehyde with the colorless 4-amino-3-hydrazino-5-mercapto-1,2,4-triazole (Purpald) resulting in the formation of a colored oxidation end product.

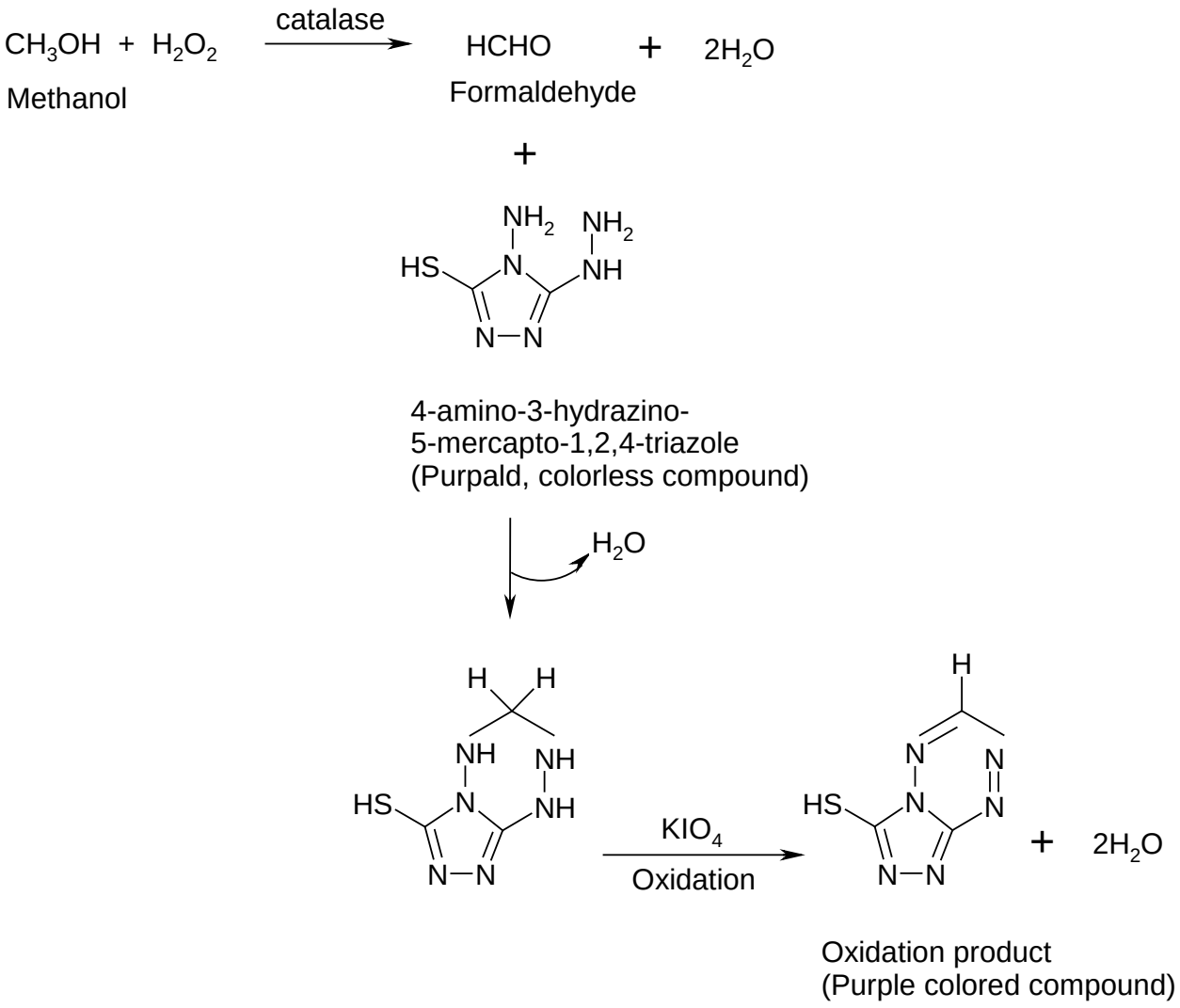

Figure 12. Structural representation of (A) O-phthaldialdehyde method and (B) DTNB (5,5-dithio-bis(2-nitro benzoic acid) method for the measurement of glutathione activity.

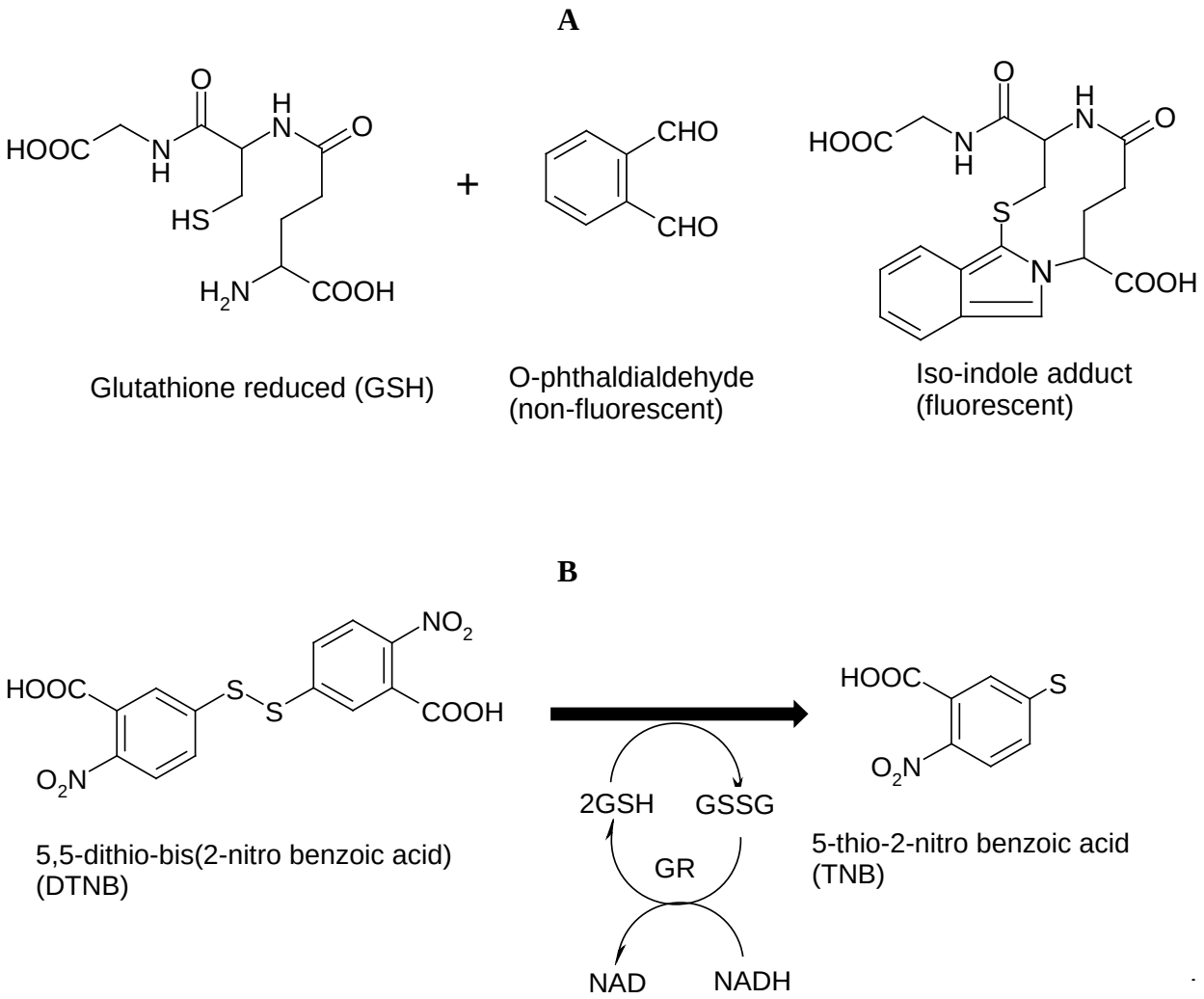

Figure 13. Structural representation of the assessment of lipid peroxidation by reacting the lipid peroxidation product Malondialdehyde with 2-thiobarbutyric acid to result in the formation of red coloured adduct which can be quantified using colorimetry.

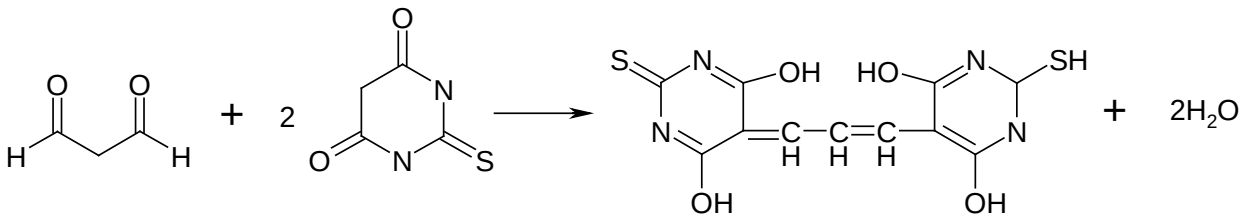

Malondialdehyde (MDA)

2-thiobarbutyric acid (TBA)

MDA:TBA adduct

Figure 14. Structural representation of the conversion of 2'-deoxyguanosine to 8-hydroxyl-2'-deoxyguanosine (8-OHdG) and its detection using ELISA assay for the identification of DNA base modifications in nanoparticles-treated cells

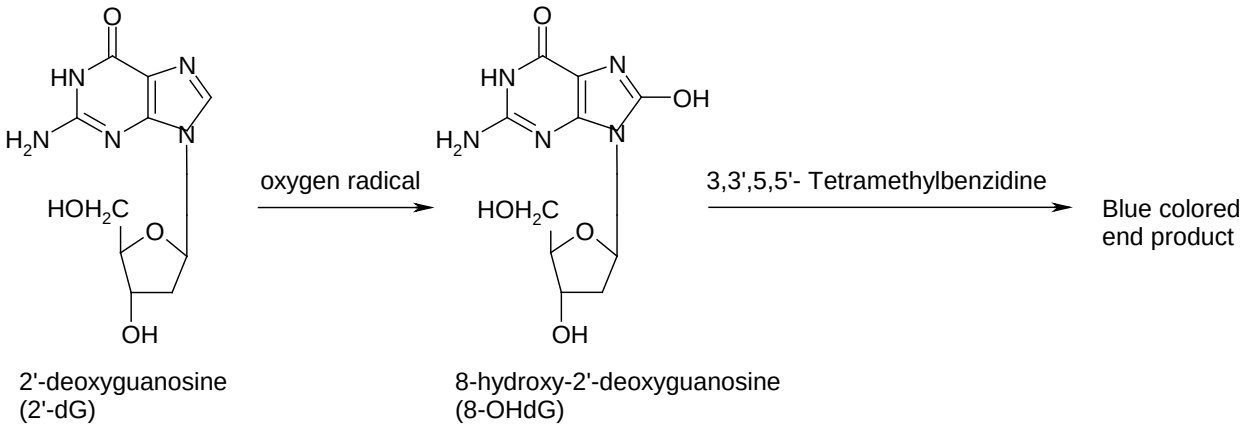

Figure 15. Schematic representation of the hemolysis assay *in vitro* for the assessment of nanoparticles-mediated blood compatibility

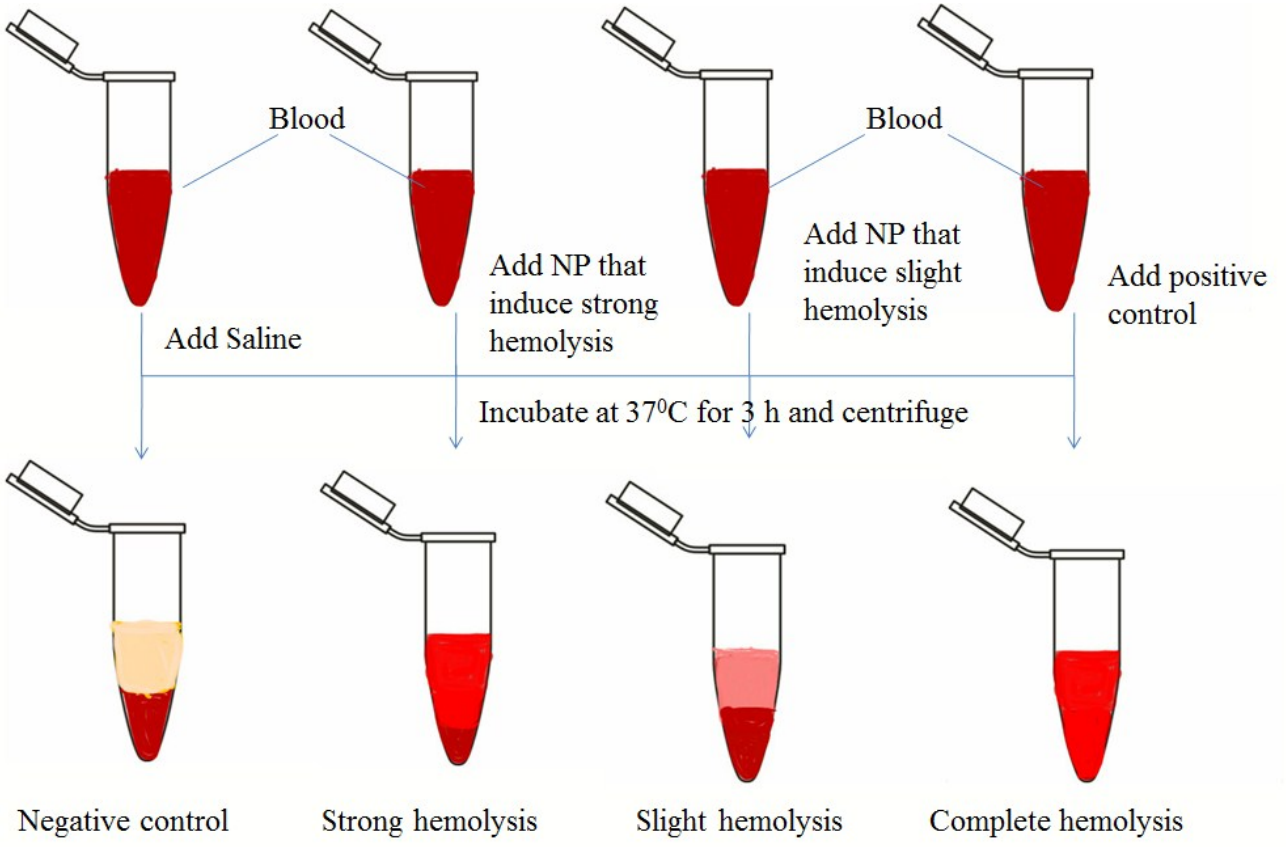

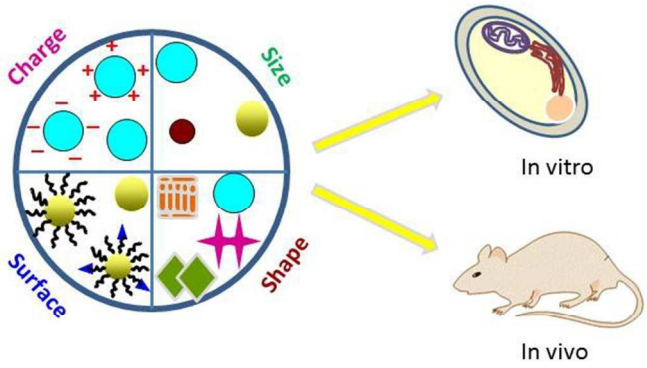

Understanding of interplay between nanoparticles' physicochemistry and biophysical properties, and their impact on pharmacokinetics biodistribution and toxicological properties, could allow designing of appropriate nanoparticles products for biomedical applications to human or veterinary use.

254x190mm (96 x 96 DPI)